Supporting Information for

Synthetic Enzyme-Catalyzed Multicomponent Reaction for Isoxazol-5(4*H*)-one Syntheses, their Properties and Biological Application. Why to Study Mechanisms?

Gabriela H. C. Oliveira,[a] Luciana M. Ramos,[a]* Raíssa K. C. de Paiva,[a] Saulo T. A. Passos,[b] Marina M. Simões,[c] Fabricio Machado,[b,d] and Marina M. Simões,[b] José R. Correa,[b] Brenno A. D. Neto,[b]*

[a] Laboratório de Química Medicinal e Síntese Orgânica (LaQuiMeSO), Câmpus de Ciências Exatas e Tecnológicas, Universidade Estadual de Goiás, CP 459, Anápolis-GO, Brasil. E-mail: luciana.ramos@ueg.br

[b] Laboratory of Medicinal and Technological Chemistry, University of Brasília, Chemistry Institute (IQ-UnB), Campus Universitario Darcy Ribeiro, Brasília, Distrito Federal, 70904-970, Brazil. E-mail: brenno.ipi@gmail.com

[c] Laboratório de Microscopia e Microanálise, Departamento de Biologia Celular, Instituto de Ciências Biológicas, Universidade de Brasília, Brasília, DF, Brasil.

[d] School of Chemistry, University of Nottingham, University Park, Nottingham, NG7 2RD, UK.

Summary

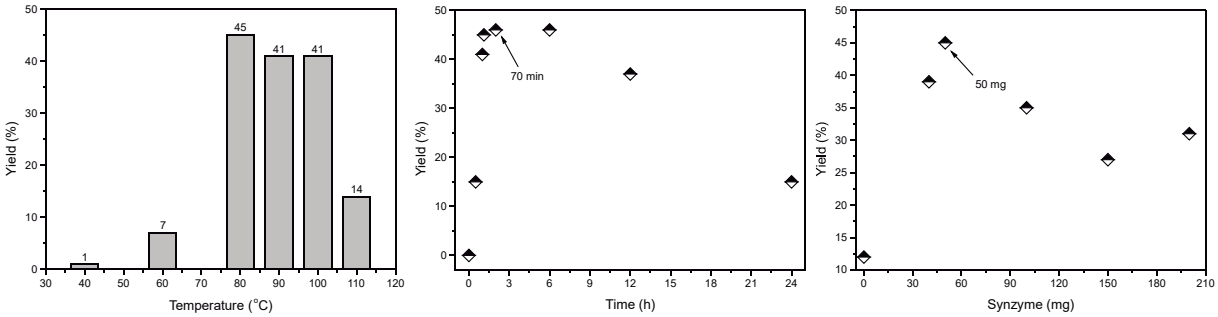

Figure S1. Reaction time, catalyst amount and temperature optimization for **ISX 01** synthesis using **PEI-IL** as the synthetic enzyme.

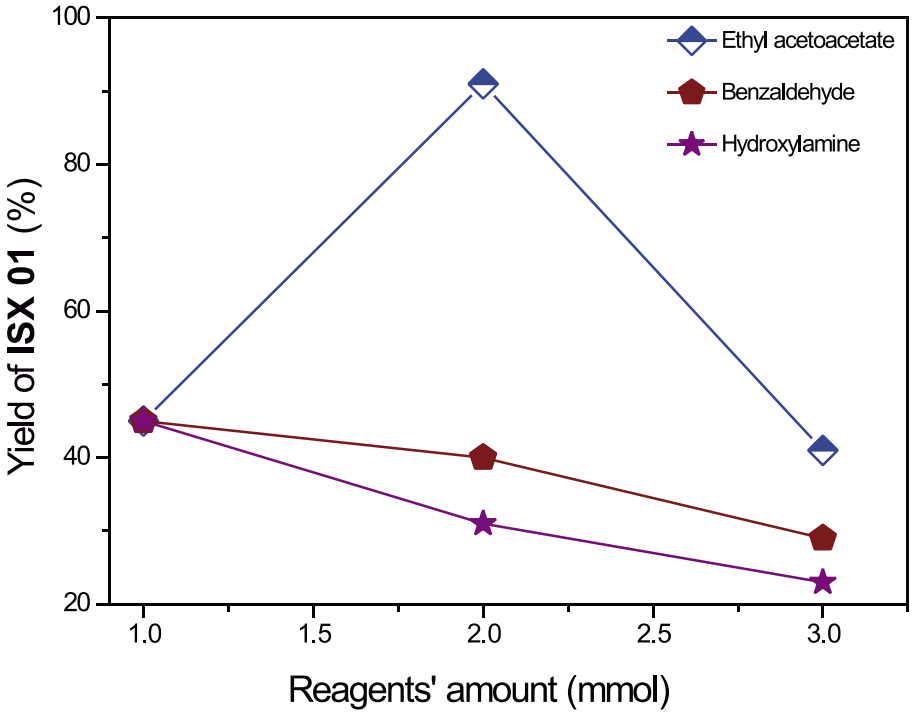

Figure S2. Reagents' concentration variation effect for the synthesis of **ISX 01** using **PEI-IL** (50 mg) as the catalyst in aqueous medium (4 mL), at 80 °C for 70 min.

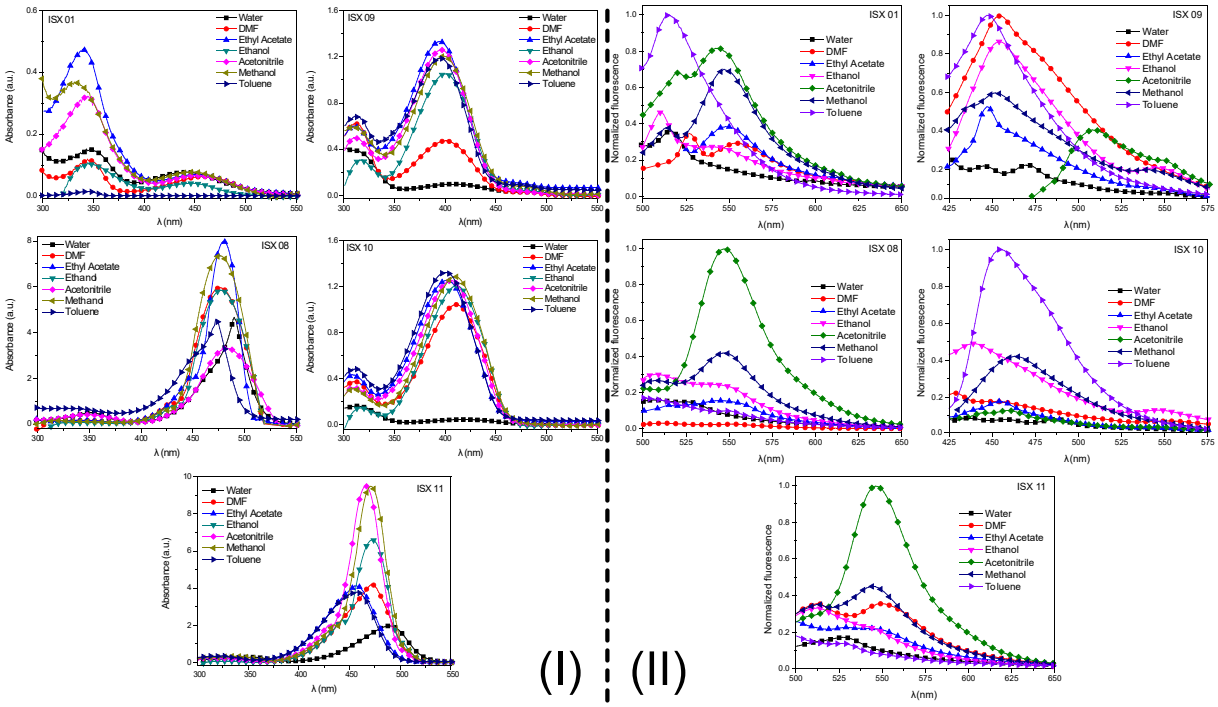

Figure S3. Photophysical analyses (10 μM for all compounds). (I) UV-Vis and (II) fluorescence emission for ISX derivatives (**ISX 01**, **ISX 08**, **ISX 09**, **ISX 10**, **ISX 11**).

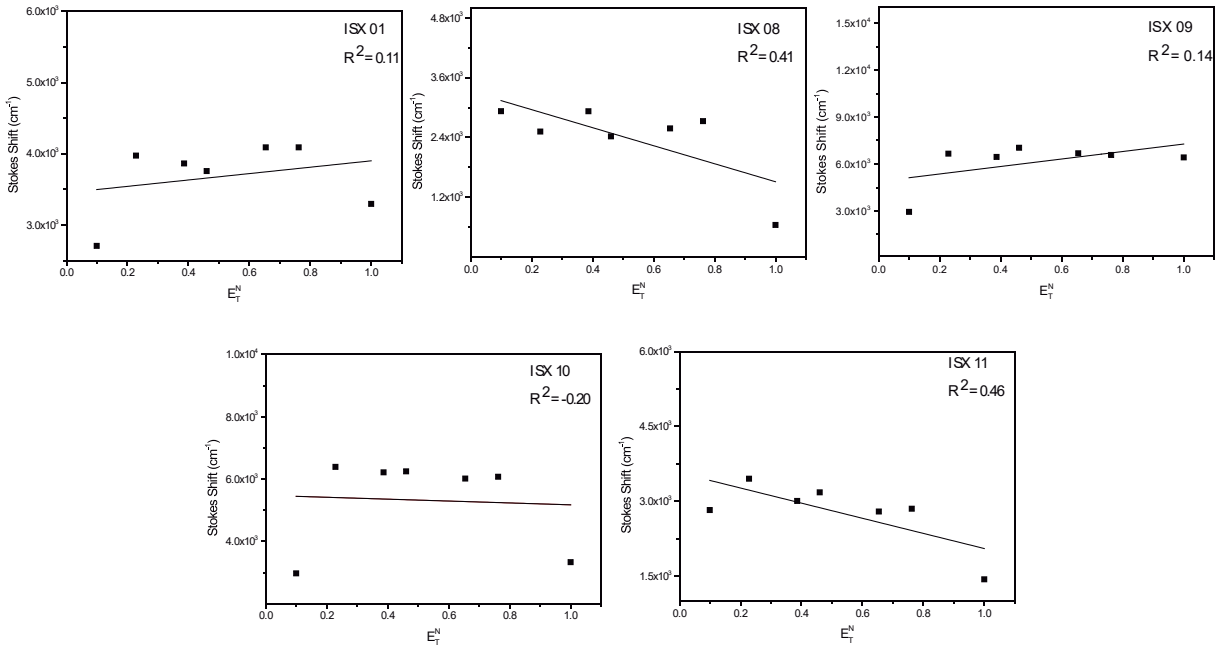

Figure S4. Solvatochromic effect (E_T^N vs. cm^{-1}) for ISX derivatives (**ISX 01**, **ISX 08**, **ISX 09**, **ISX 10**, **ISX 11**).

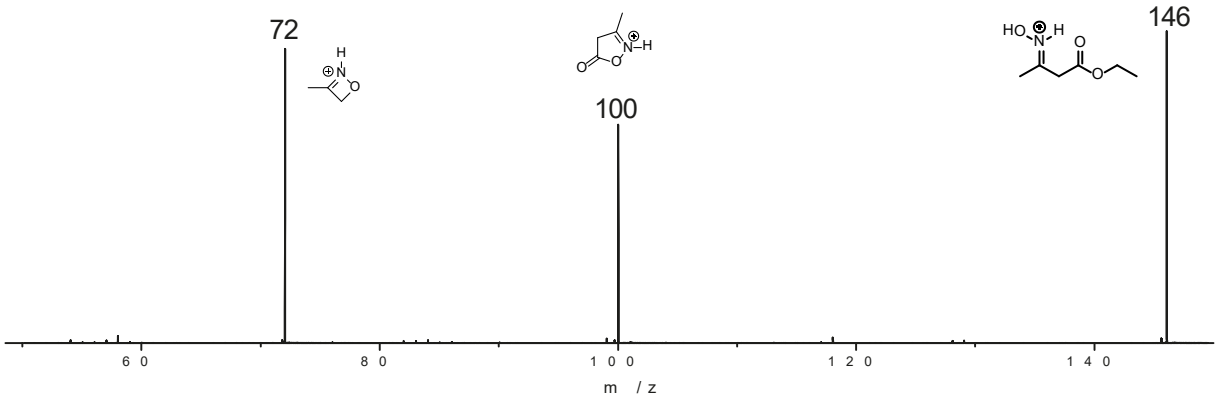

Figure S5. ESI(+)-MS/MS of the signal of *m/z* 146.

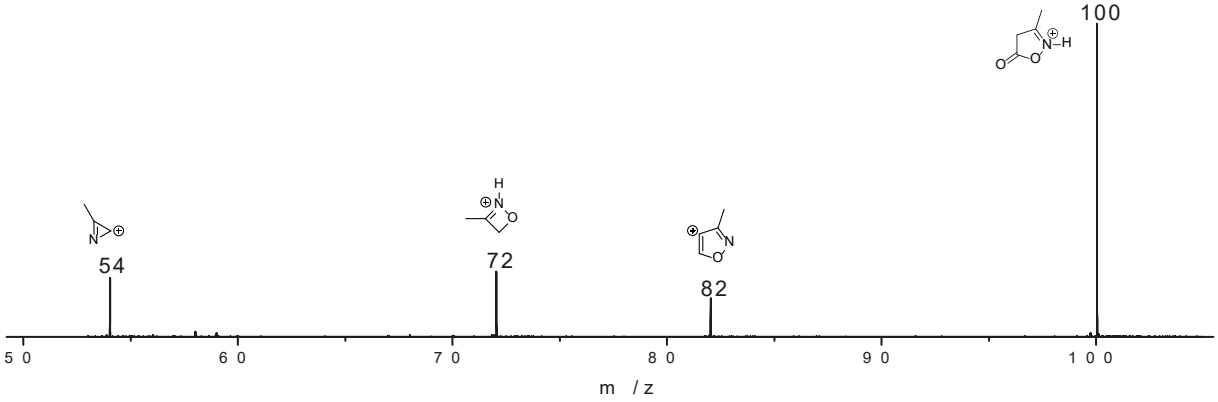

Figure S6. ESI(+)-MS/MS of the signal of *m/z* 100.

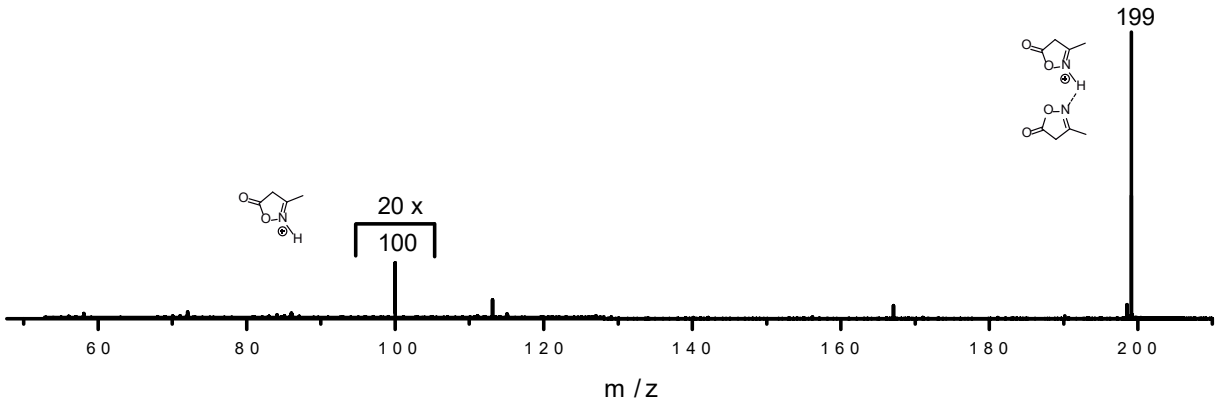

Figure S7. ESI(+)-MS/MS of the signal of *m/z* 199.

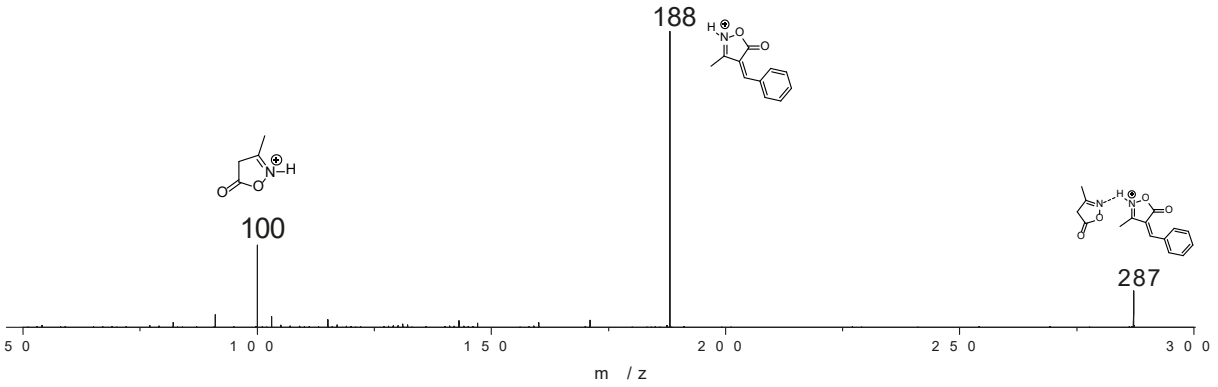

Figure S8. ESI(+)-MS/MS of the signal of *m/z* 287.

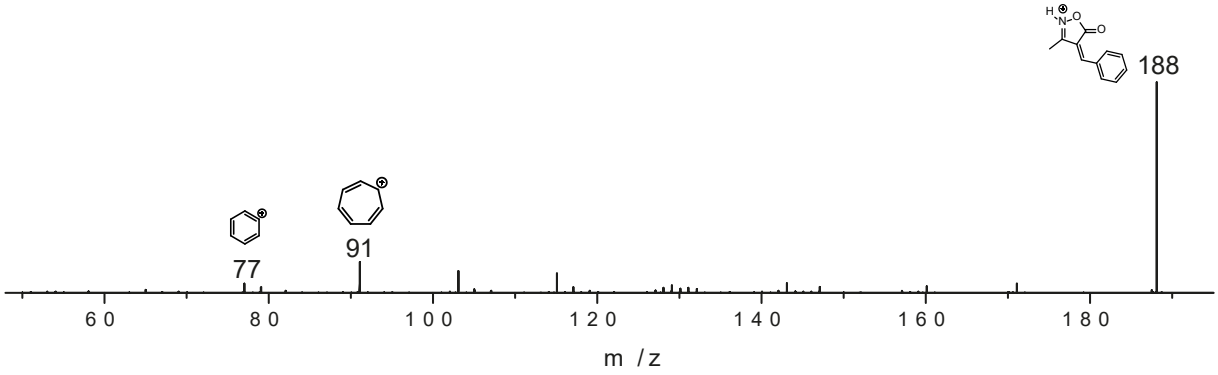

Figure S9. ESI(+)-MS/MS of the signal of *m/z* 188.

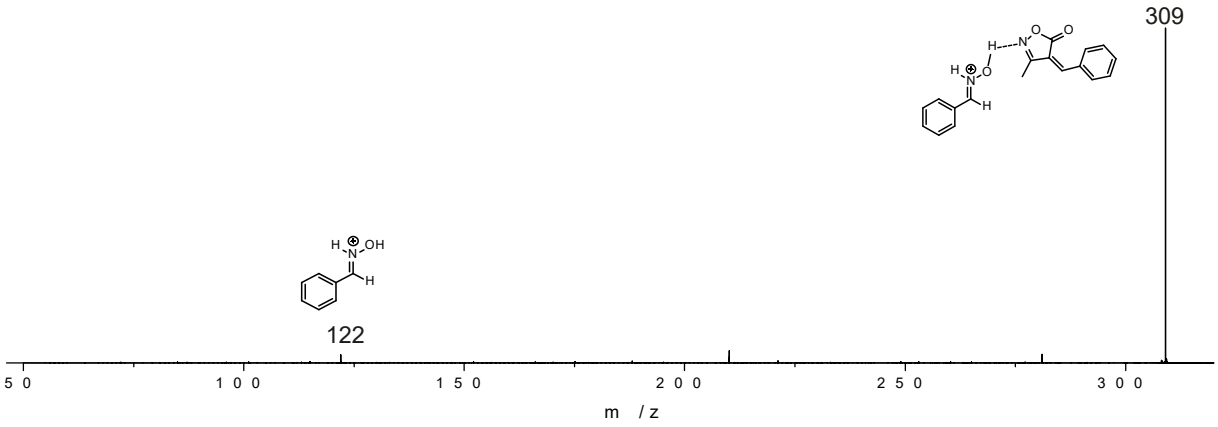

Figure S10. ESI(+)-MS/MS of the signal of *m/z* 309.

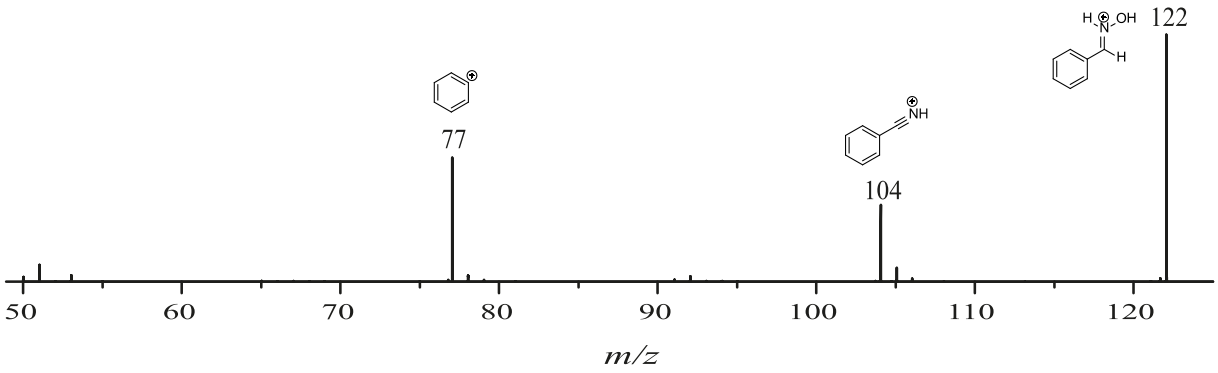

Figure S11. ESI(+)-MS/MS of the signal of *m/z* 122.

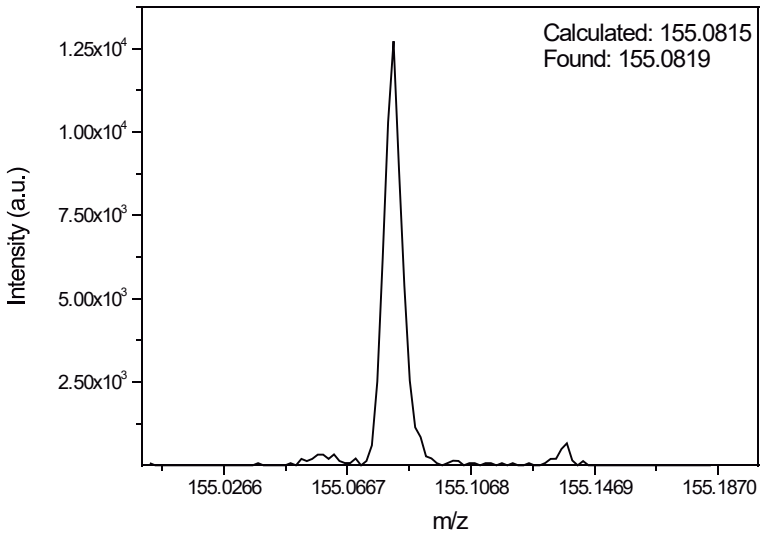

Figure S12. High resolution ESI(+)-MS showing the formation of the signal of *m/z* 155.

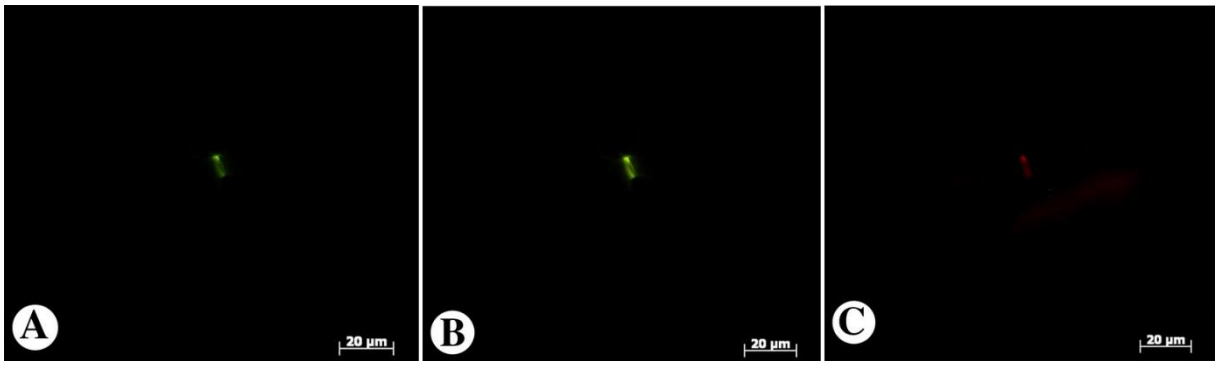

Figure S13. Walker 256 cells stained with **ISX 10**. (A), (B), and (C) show the aggregated state (crystal formation) for the ISX derivative. (A), (B), and (C) also show the symmetric aspect of the crystals by phase contrast microscopy. (A) and (B) show the green fluorescent emission from the crystal. (A) and (B) were obtained by exciting the crystal at 405 and 488 nm, respectively whereas (C) shows the red fluoresce from the crystal structure when the sample was excited at 633 nm. Scale bar of 20 μm.

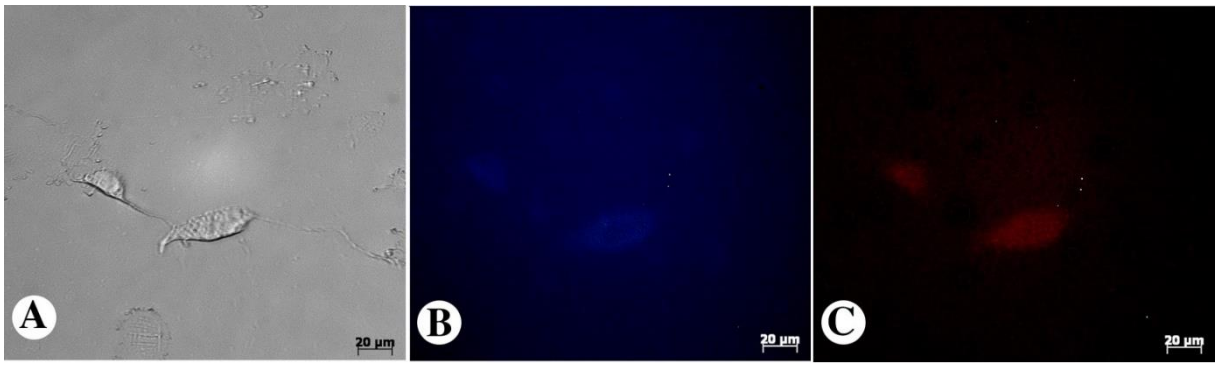

Figure S14. Walker 256 cells stained with **ISX 09**. (A) shows the phase contrast microscopy. (B) shows the sample dispersed in the cytosol emitting blue when irradiated at 405 nm. (B) shows the sample dispersed in the cytosol emitting red when irradiated at 488 nm. Scale bar of 20 µm.

Table S1. Kamlet-Taft parameters.

Solvent	**π***	**β**	**α**
Water	1.09	0.47	1.17
Acetonitrile	0.66	0.31	0.19
Ethanol	0.62	0.77	0.83
Toluene	0.50	0.11	0
THF	0.55	0.55	0

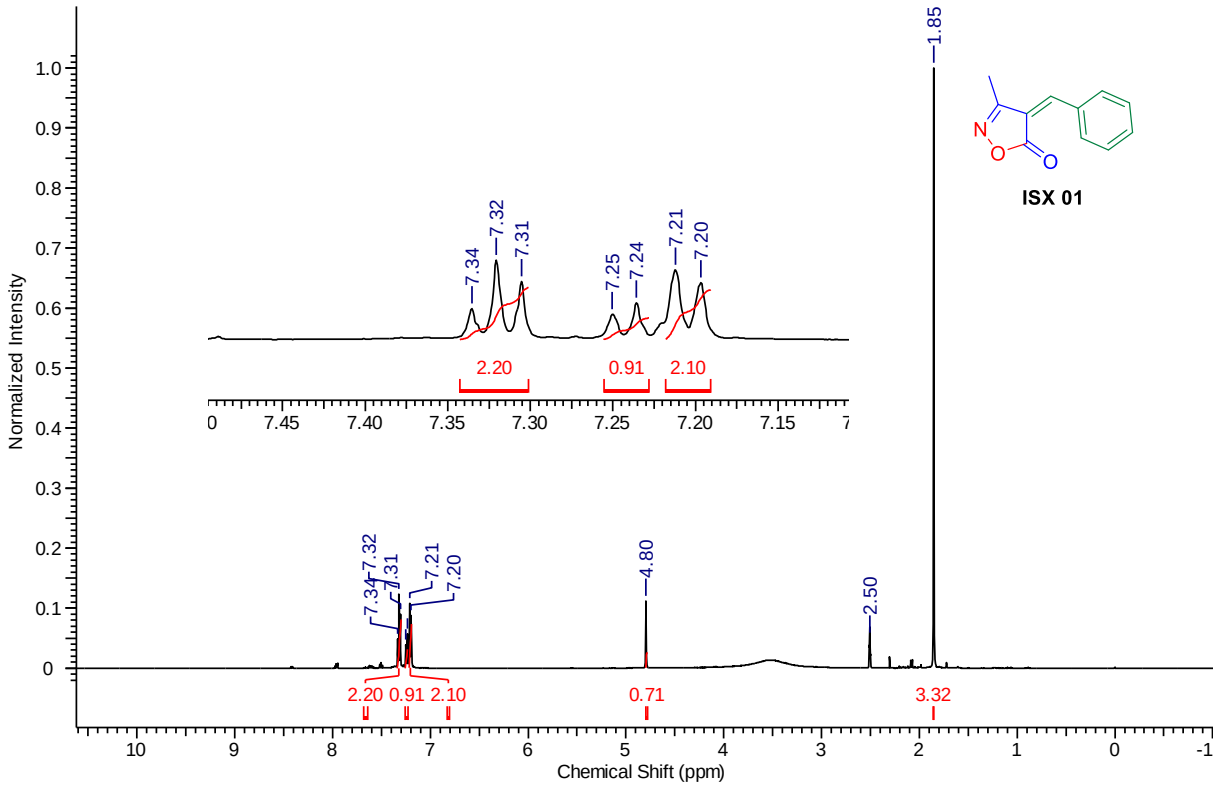

Figure S15. ^{1}H NMR spectrum (500 MHz, $CDCl_3$) of **ISX 01**.

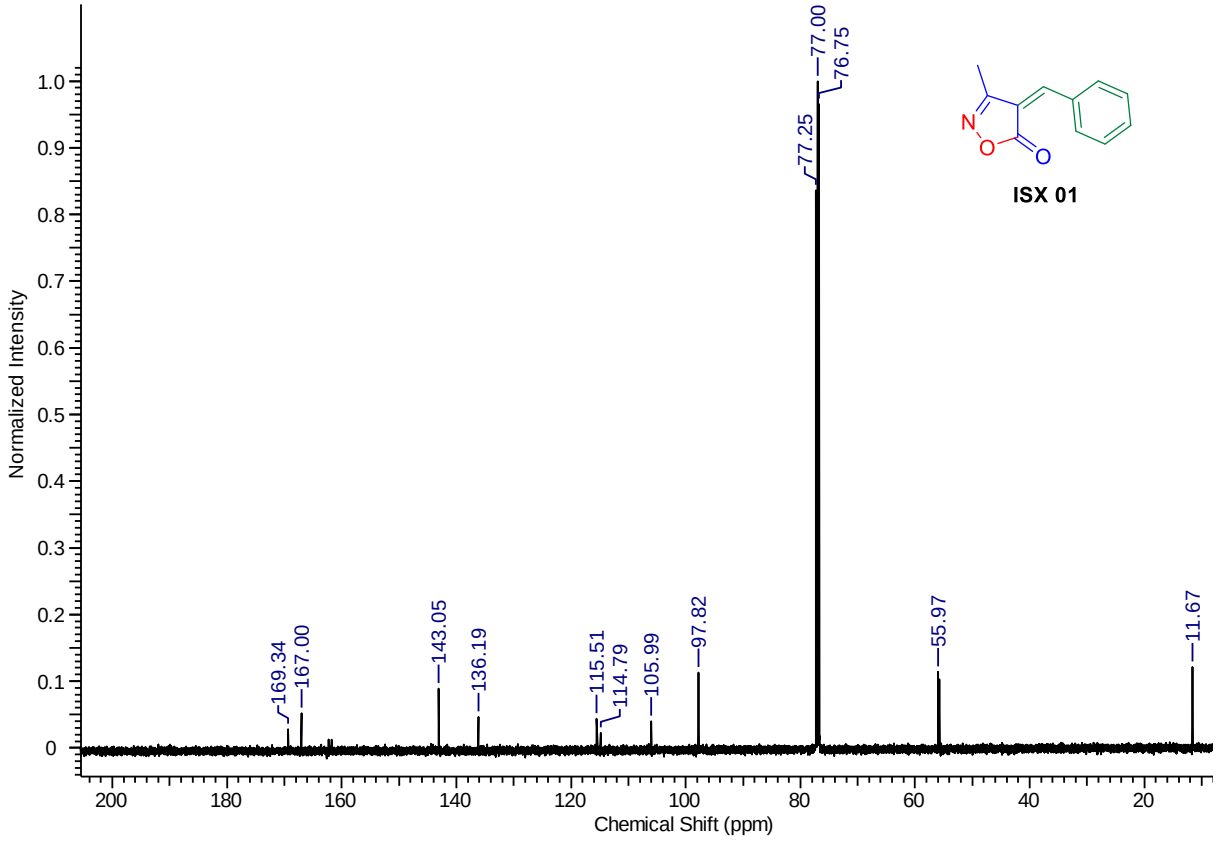

Figure S16. ^{13}C NMR spectrum (125 MHz, $CDCl_3$) of **ISX 01**.

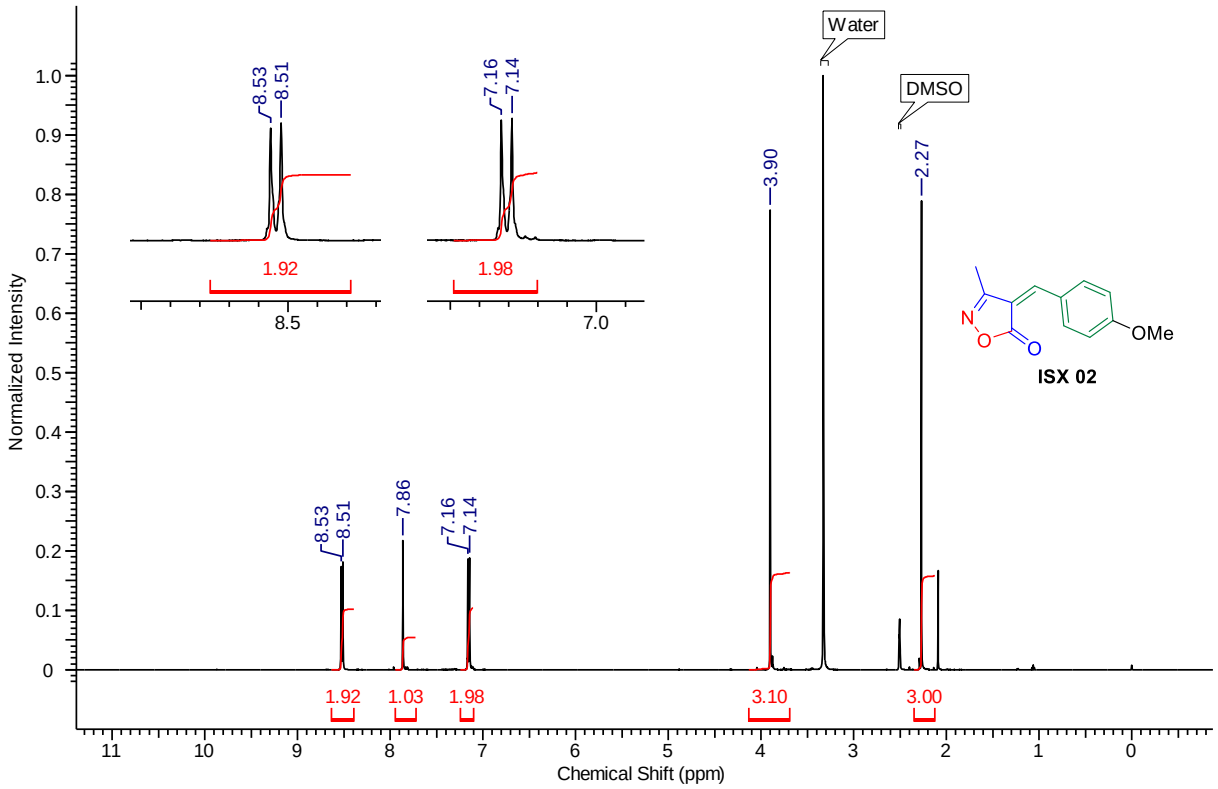

Figure S17. [1]H NMR spectrum (500 MHz, DMSO-*d6*) of **ISX 02**.

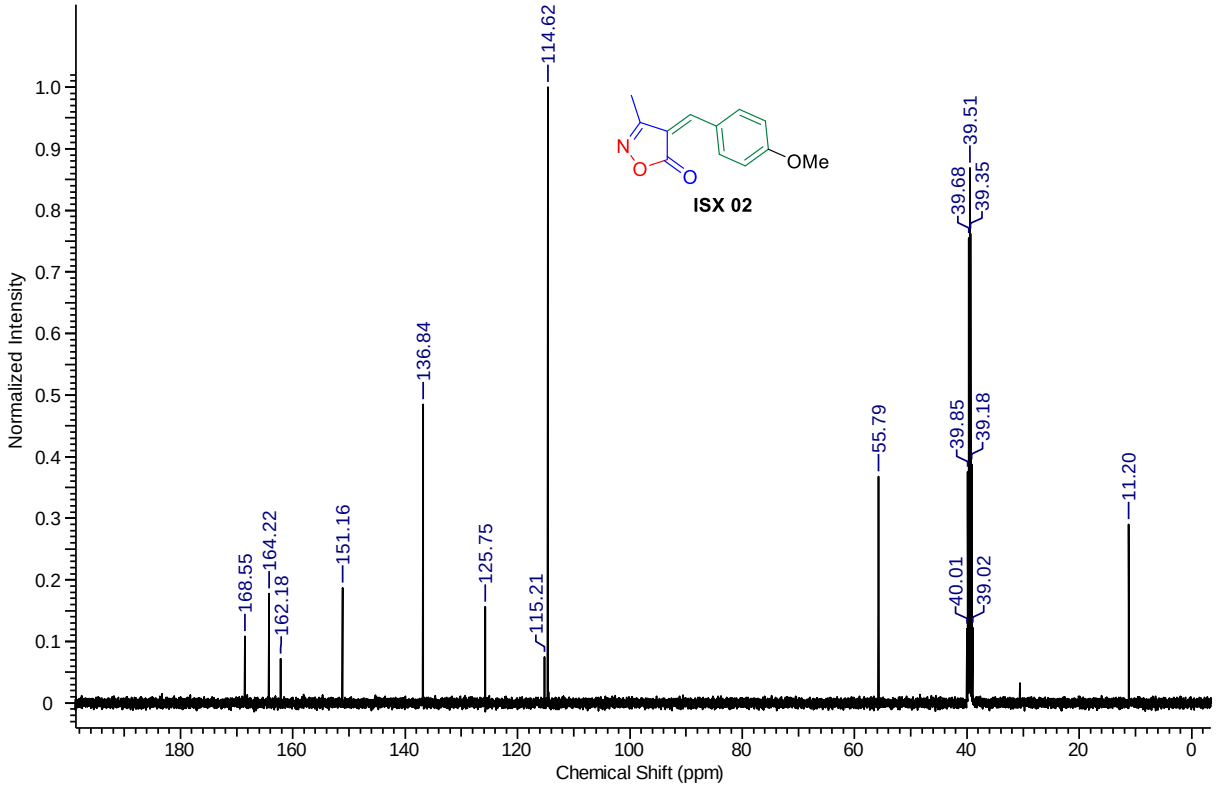

Figure S18. [13]C NMR spectrum (125 MHz, DMSO-*d6*) of **ISX 02**.

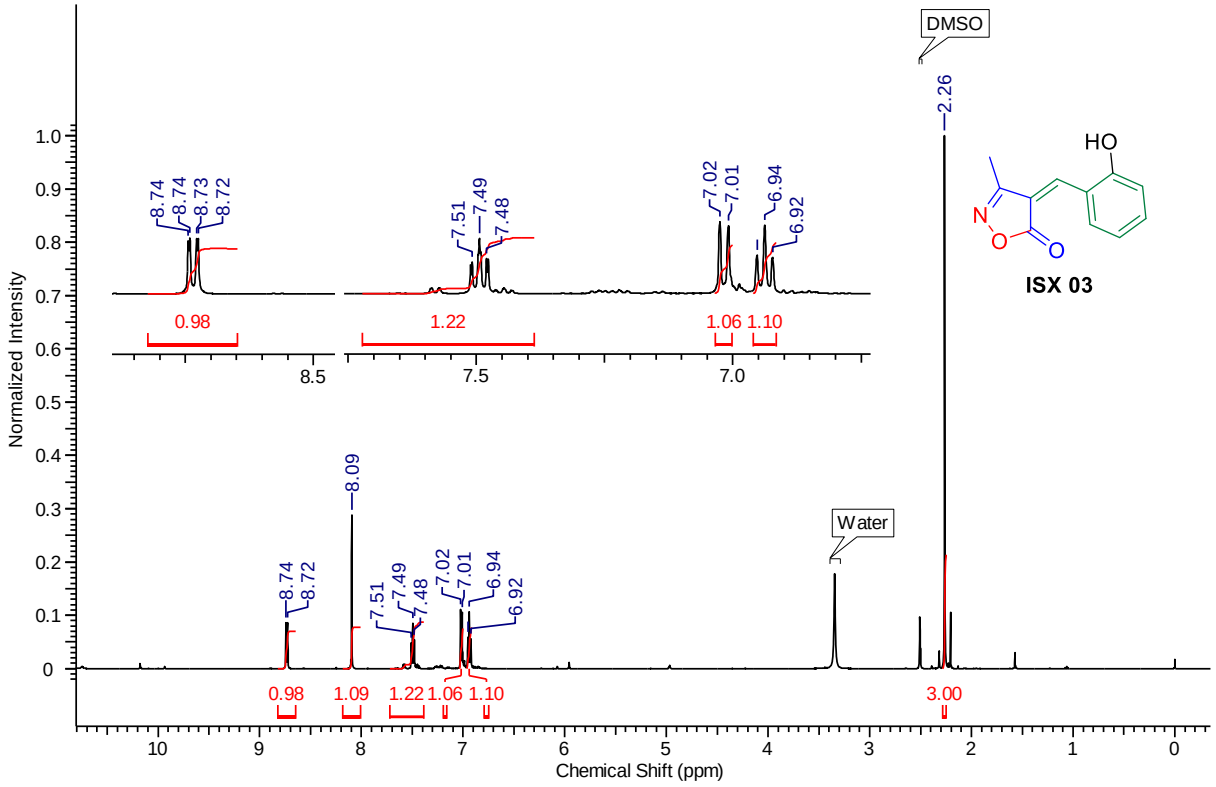

Figure S19. [1]H NMR spectrum (500 MHz, DMSO-*d6*) of **ISX 03**.

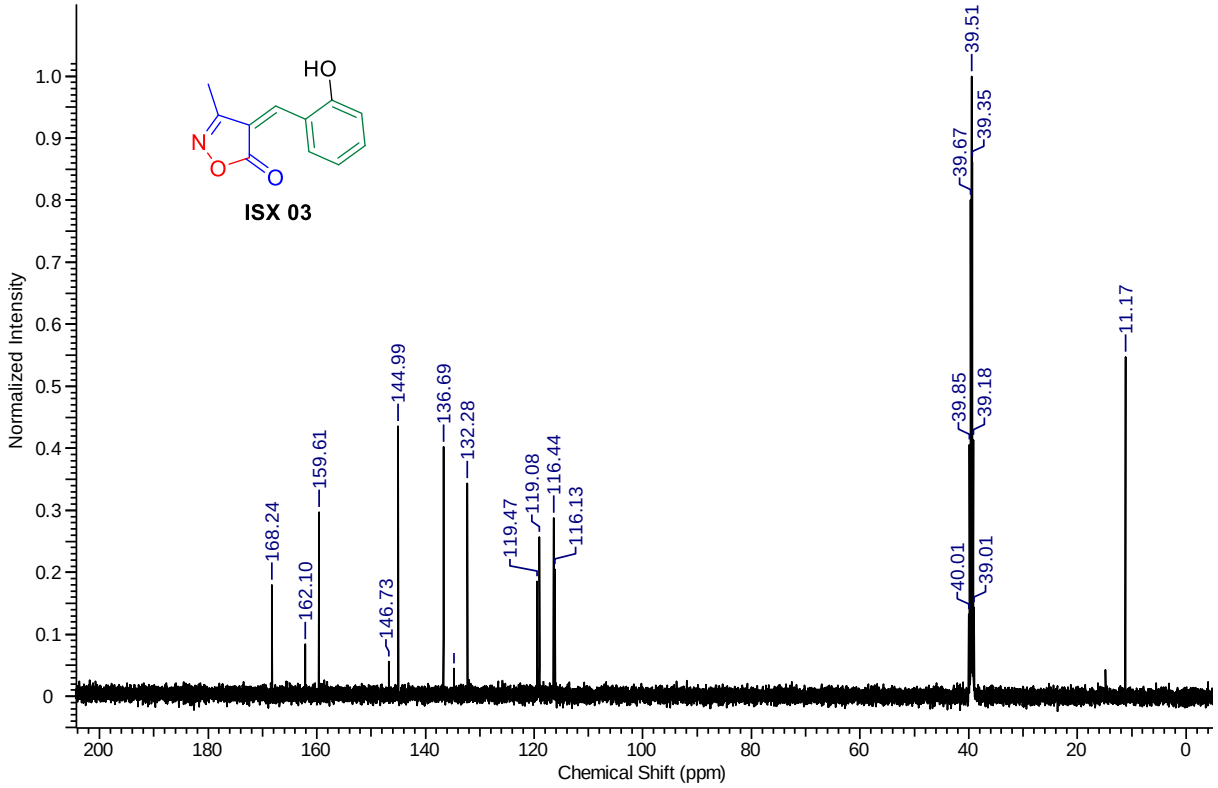

Figure S20. [13]C NMR spectrum (125 MHz, DMSO-*d6*) of **ISX 03**.

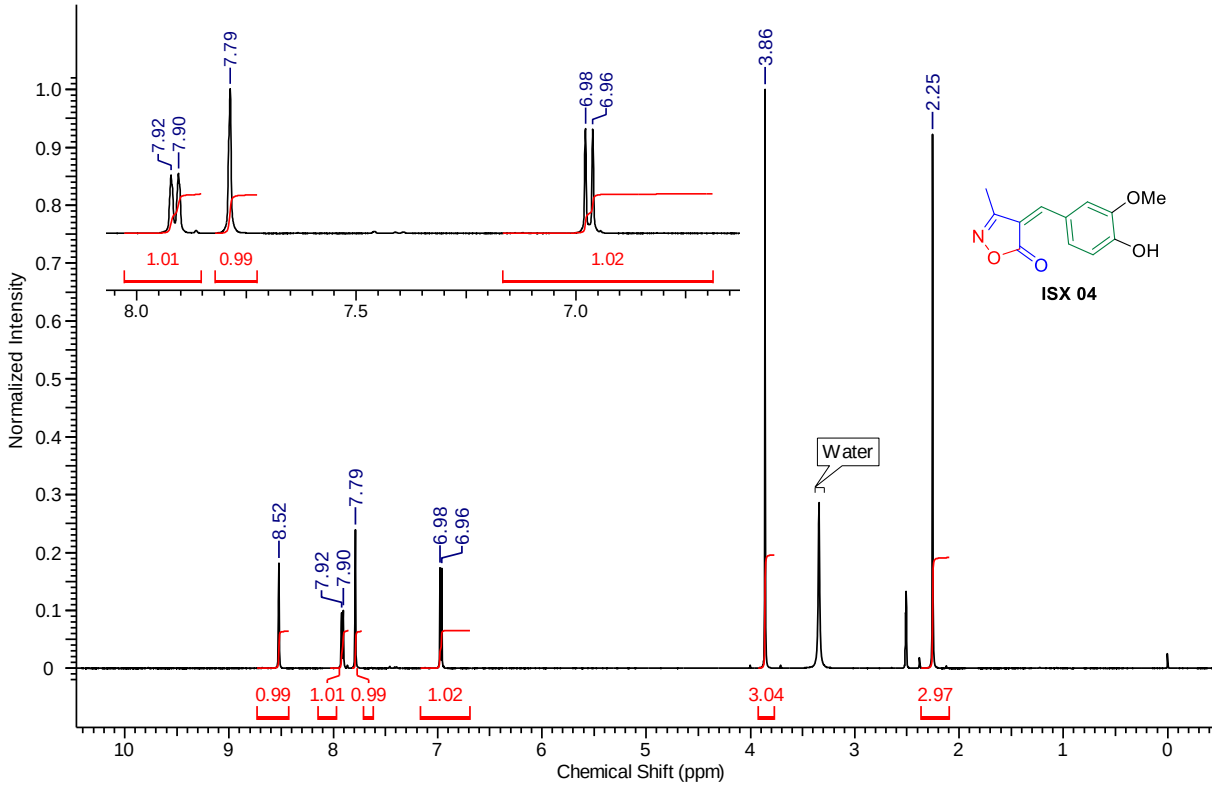

Figure S21. ^{1}H NMR spectrum (500 MHz, DMSO-*d6*) of **ISX 04**.

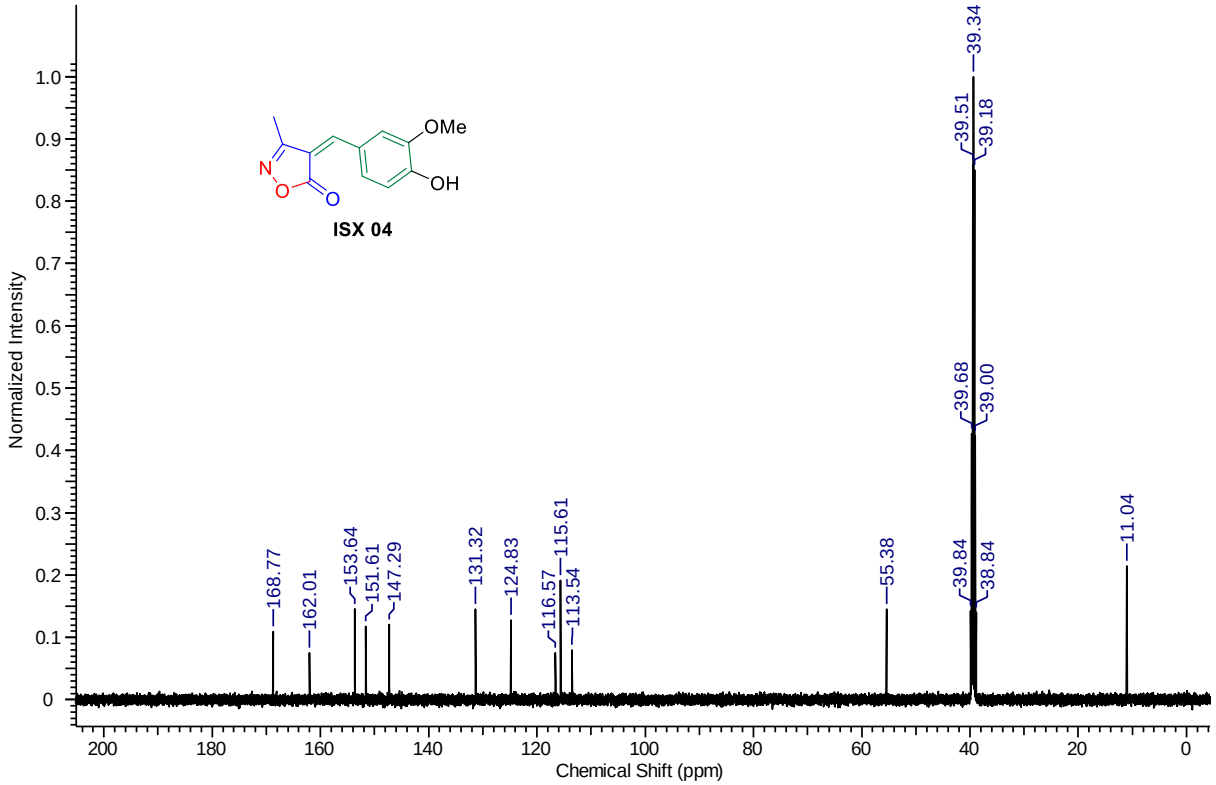

Figure S22. ^{13}C NMR spectrum (125 MHz, DMSO-*d6*) of **ISX 04**.

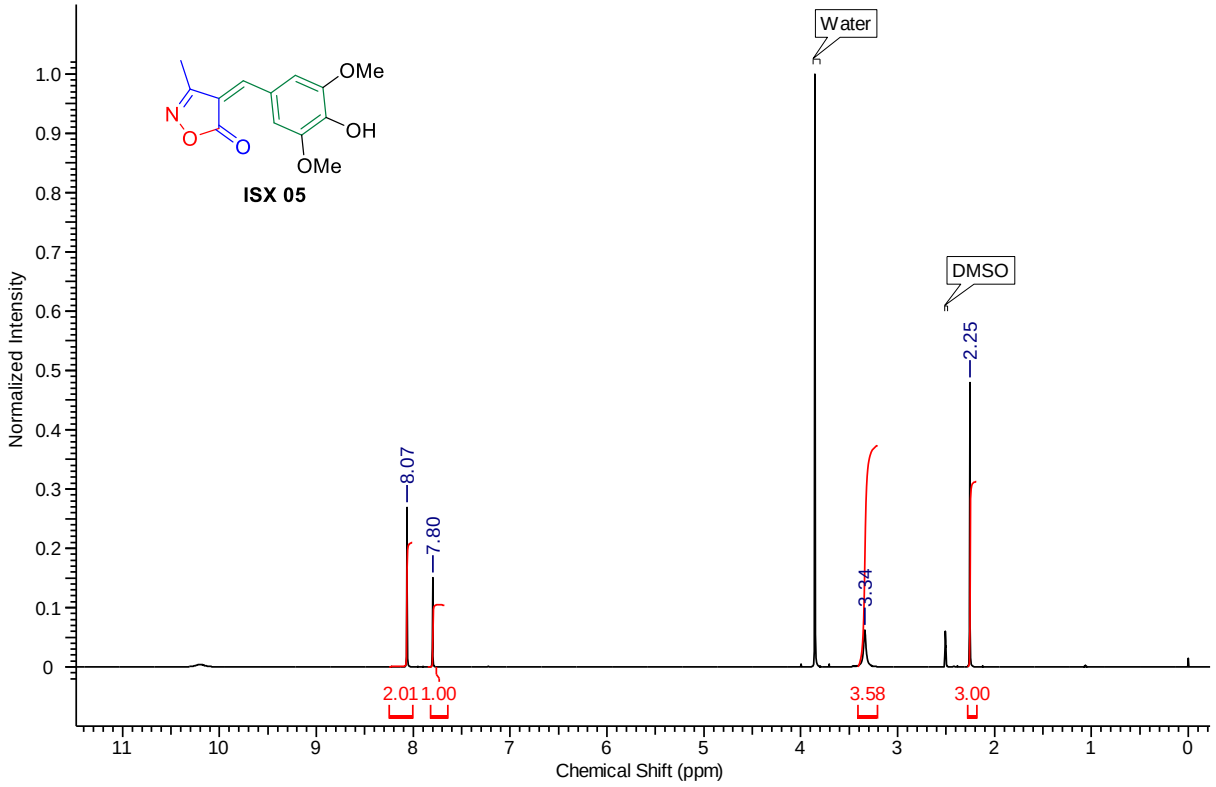

Figure S23. ^{1}H NMR spectrum (500 MHz, DMSO-*d6*) of **ISX 05**.

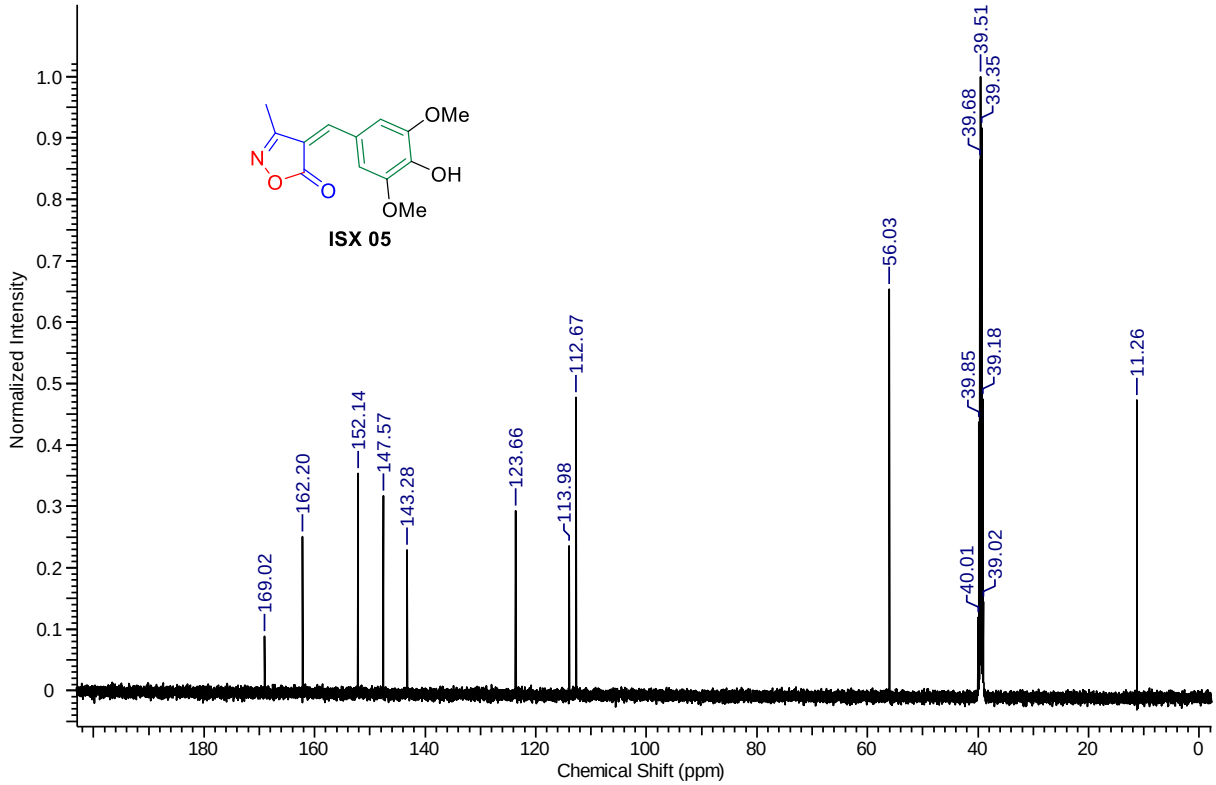

Figure S24. ^{13}C NMR spectrum (125 MHz, DMSO-*d6*) of **ISX 05**.

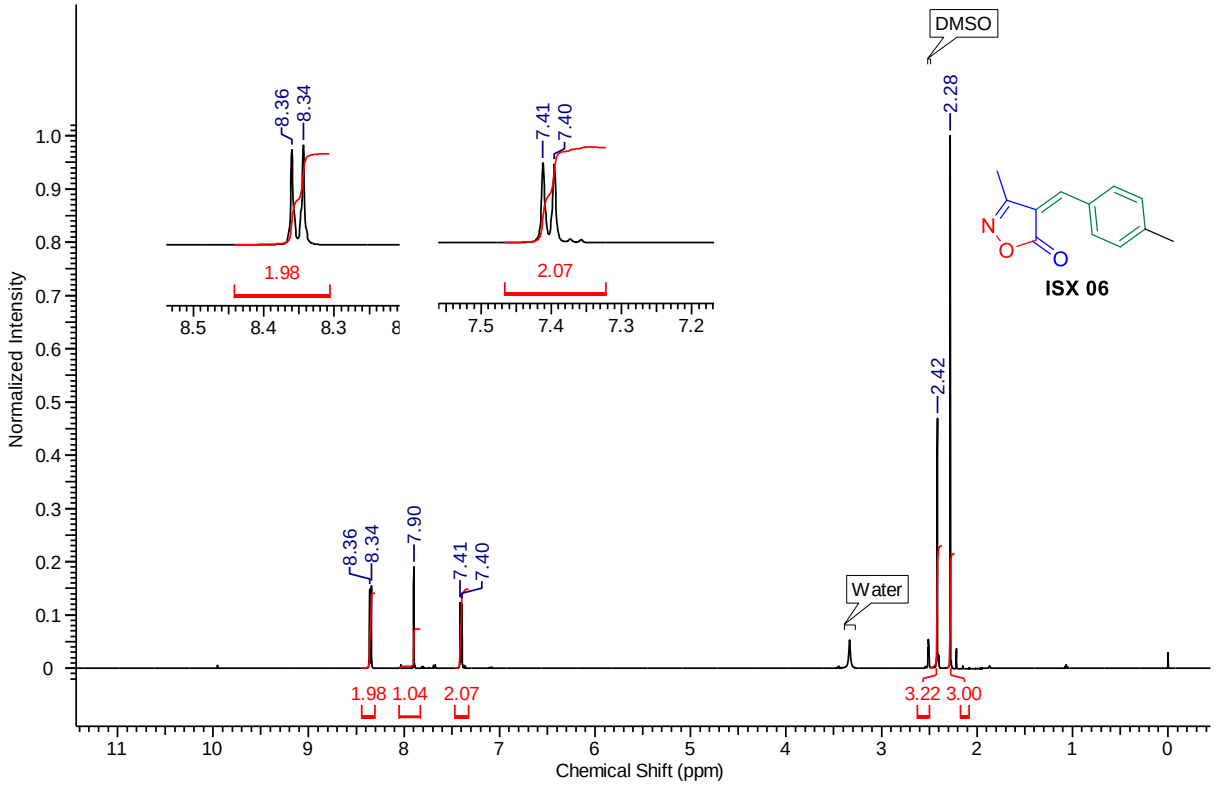

Figure S25. [1]H NMR spectrum (500 MHz, DMSO-*d6*) of **ISX 06**.

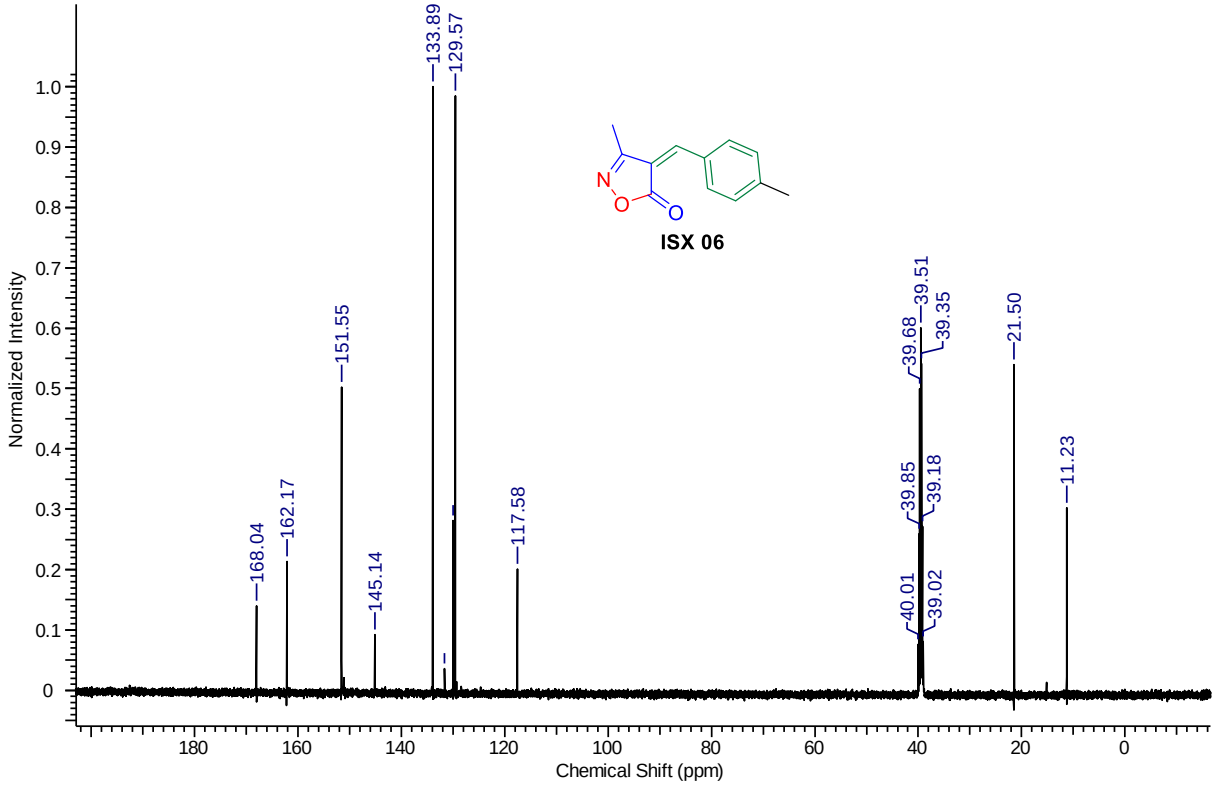

Figure S26. [13]C NMR spectrum (125 MHz, DMSO-*d6*) of **ISX 06**.

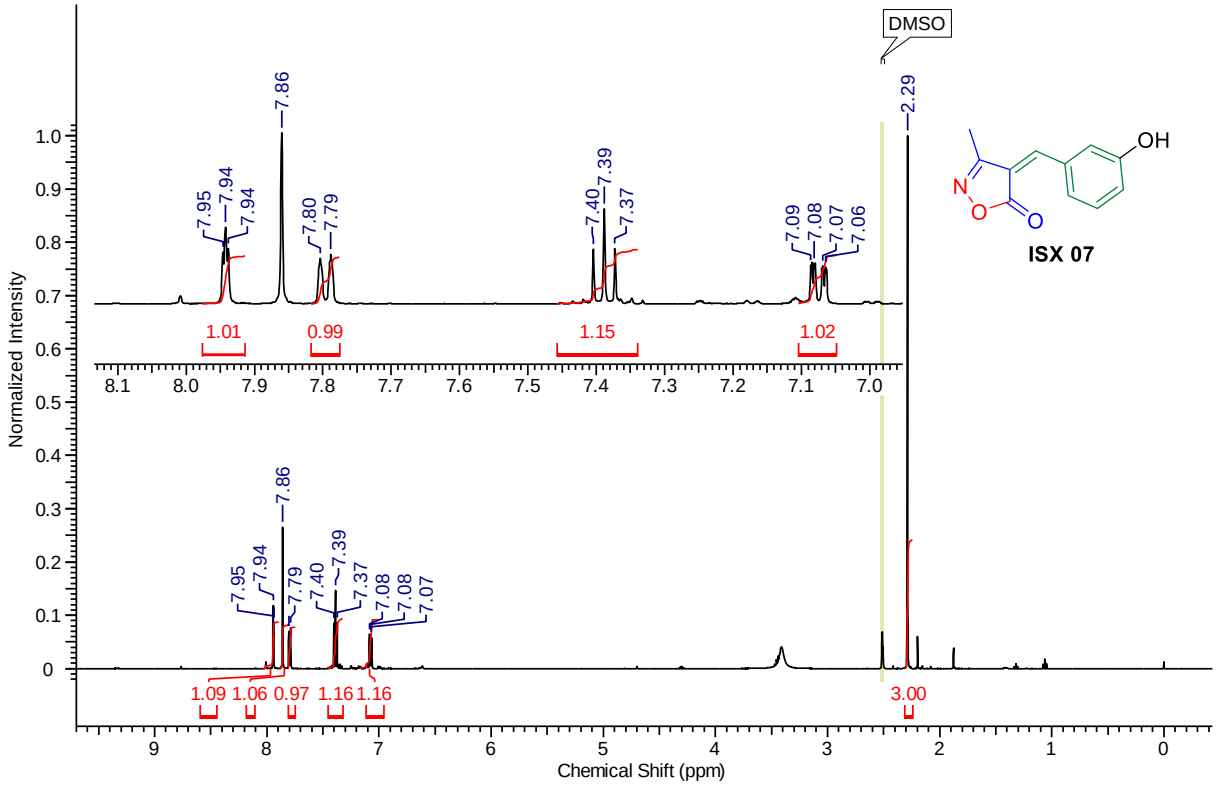

Figure S27. [1]H NMR spectrum (500 MHz, DMSO-*d6*) of **ISX 07**.

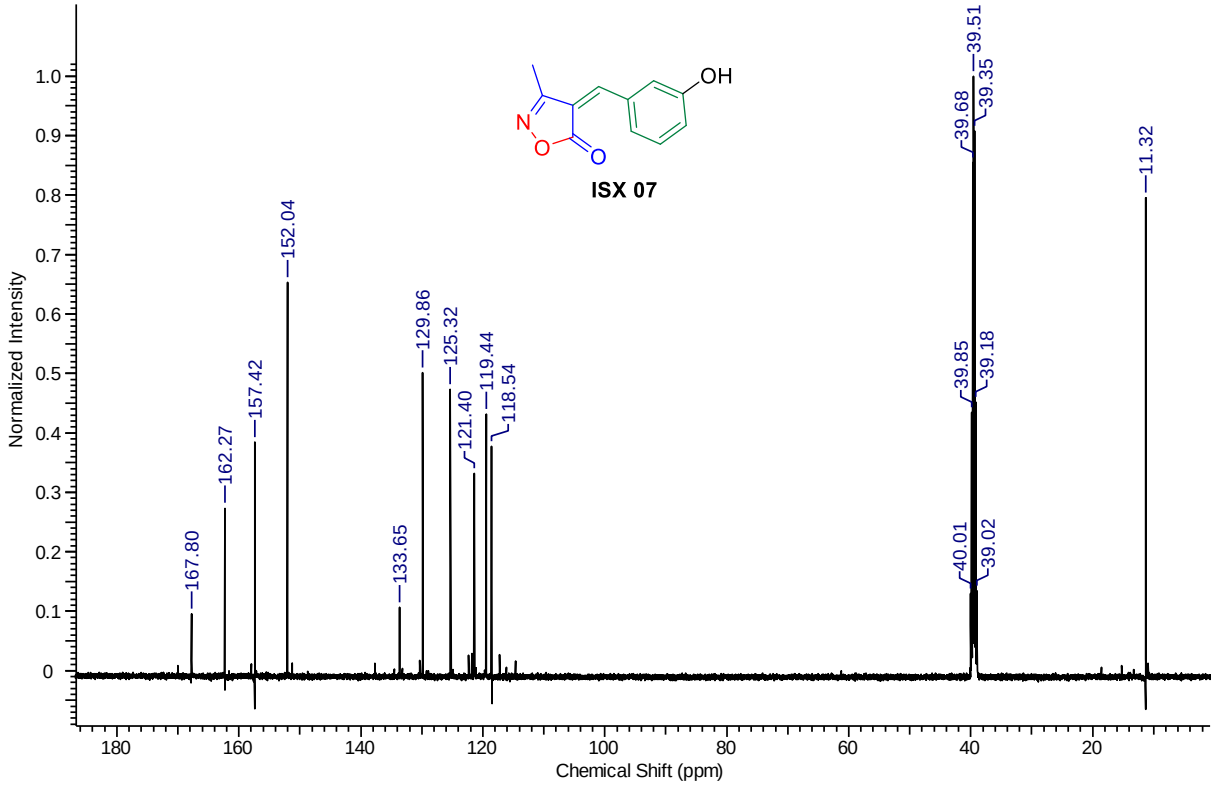

Figure S28. [13]C NMR spectrum (125 MHz, DMSO-*d6*) of **ISX 07**.

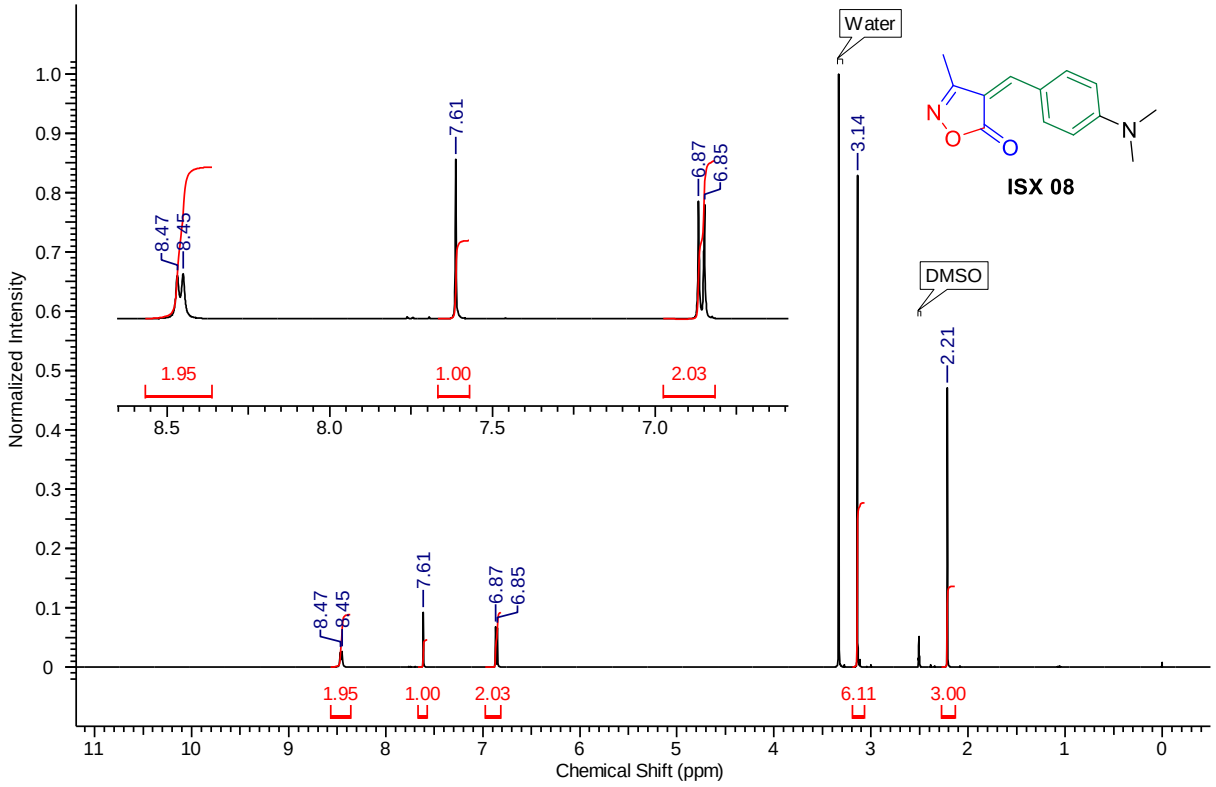

Figure S29. [1]H NMR spectrum (500 MHz, DMSO-*d6*) of **ISX 08**.

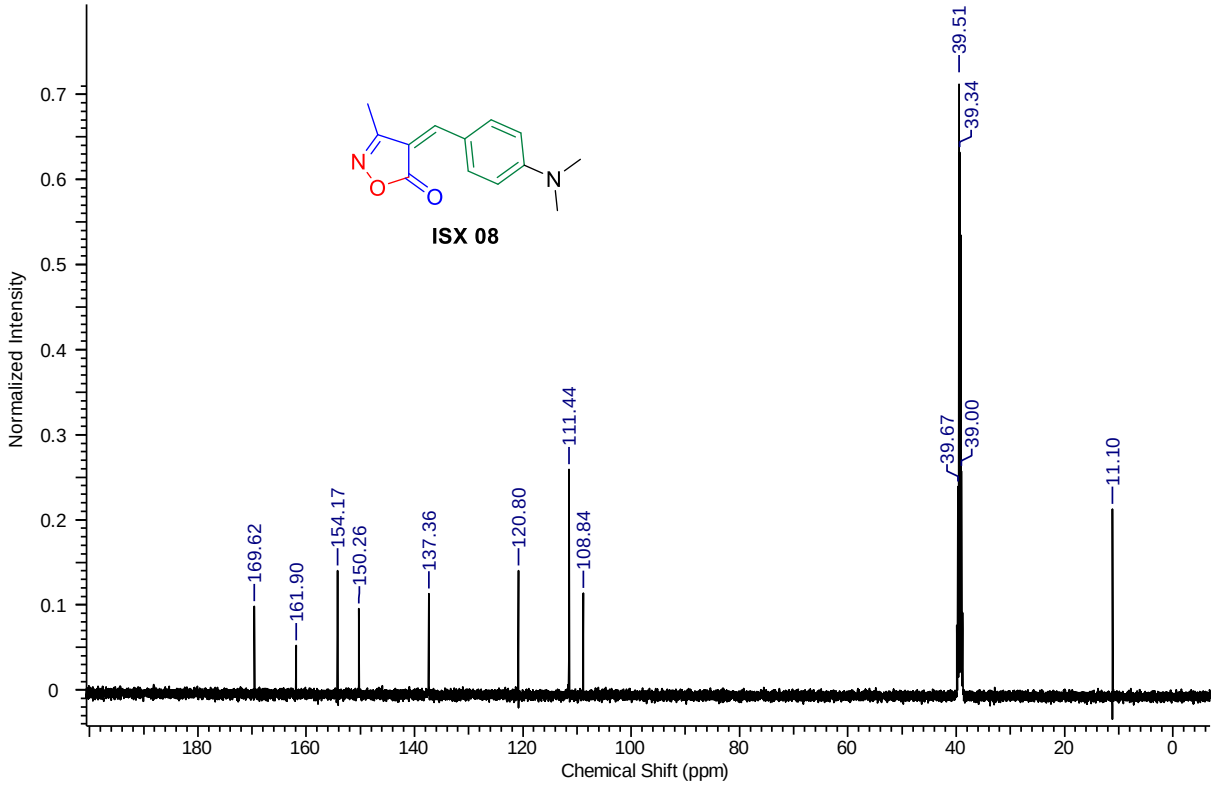

Figure S30. [13]C NMR spectrum (125 MHz, DMSO-*d6*) of **ISX 08**.

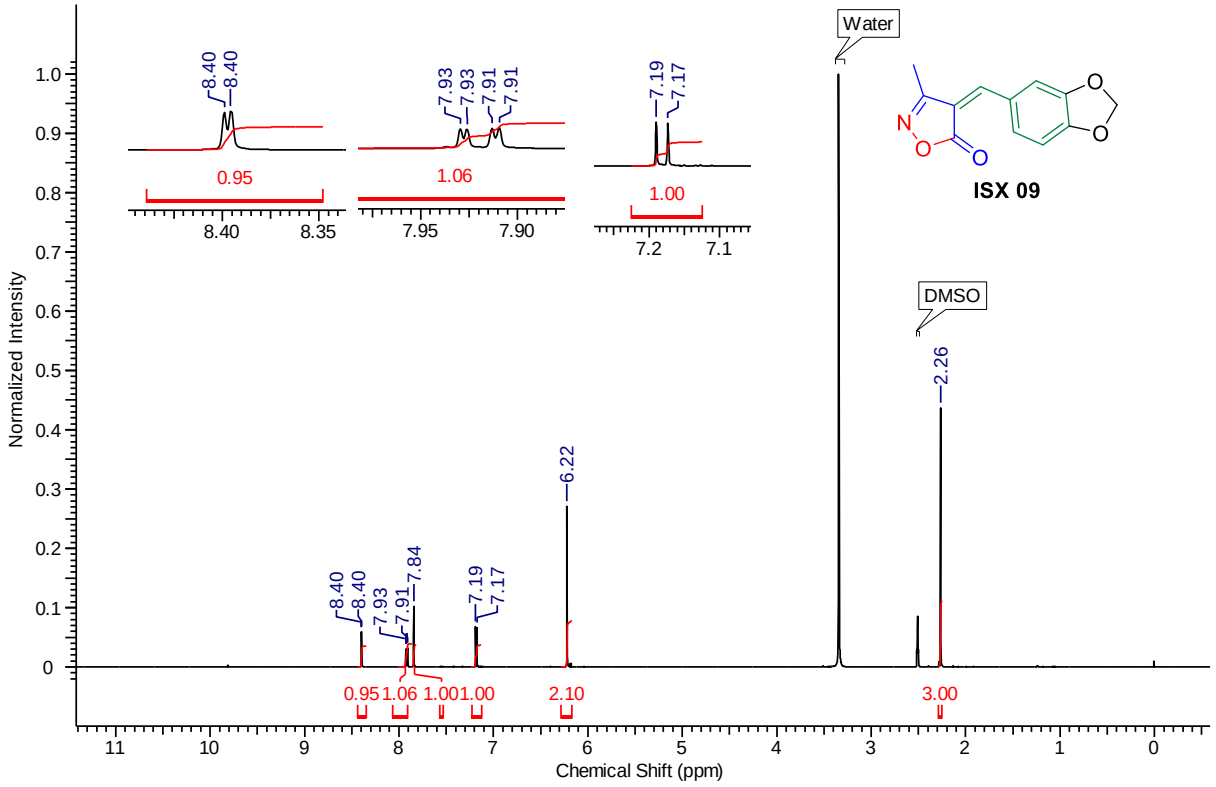

Figure S31. [1]H NMR spectrum (500 MHz, DMSO-*d6*) of **ISX 09**.

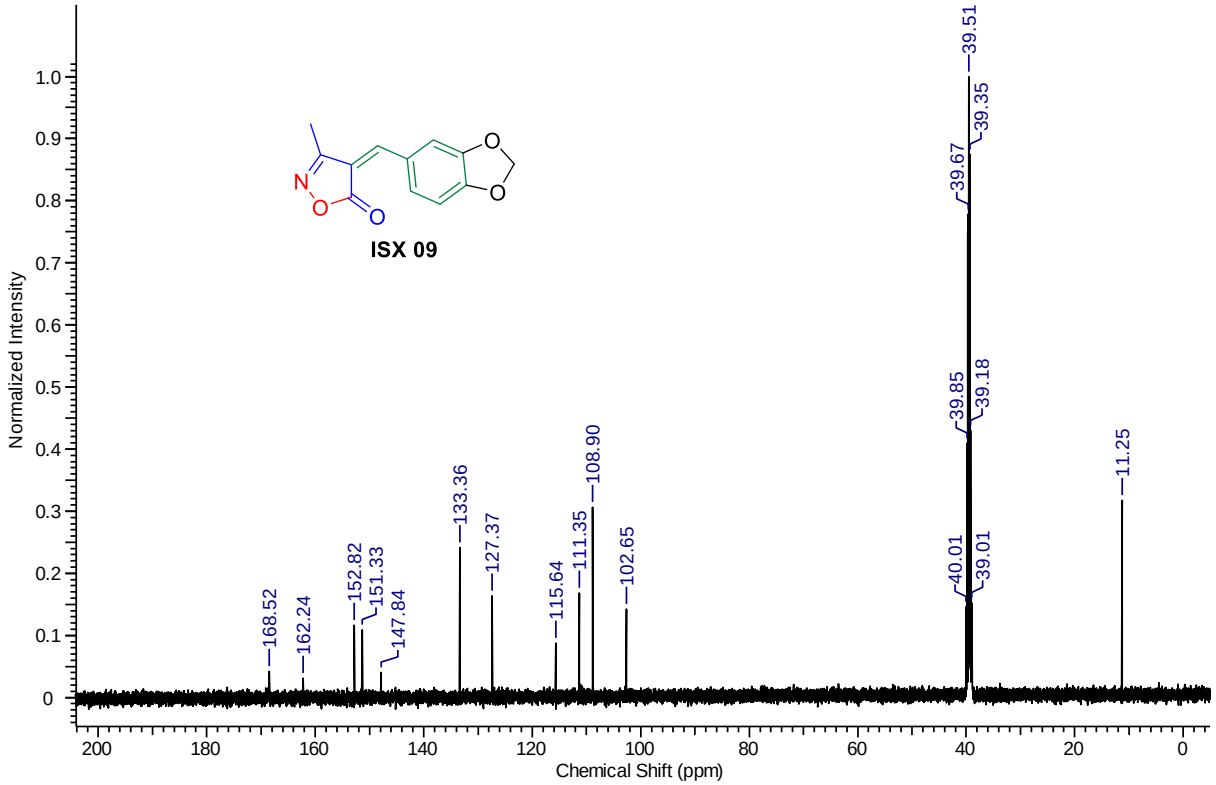

Figure S32. [13]C NMR spectrum (125 MHz, DMSO-*d6*) of **ISX 09**.

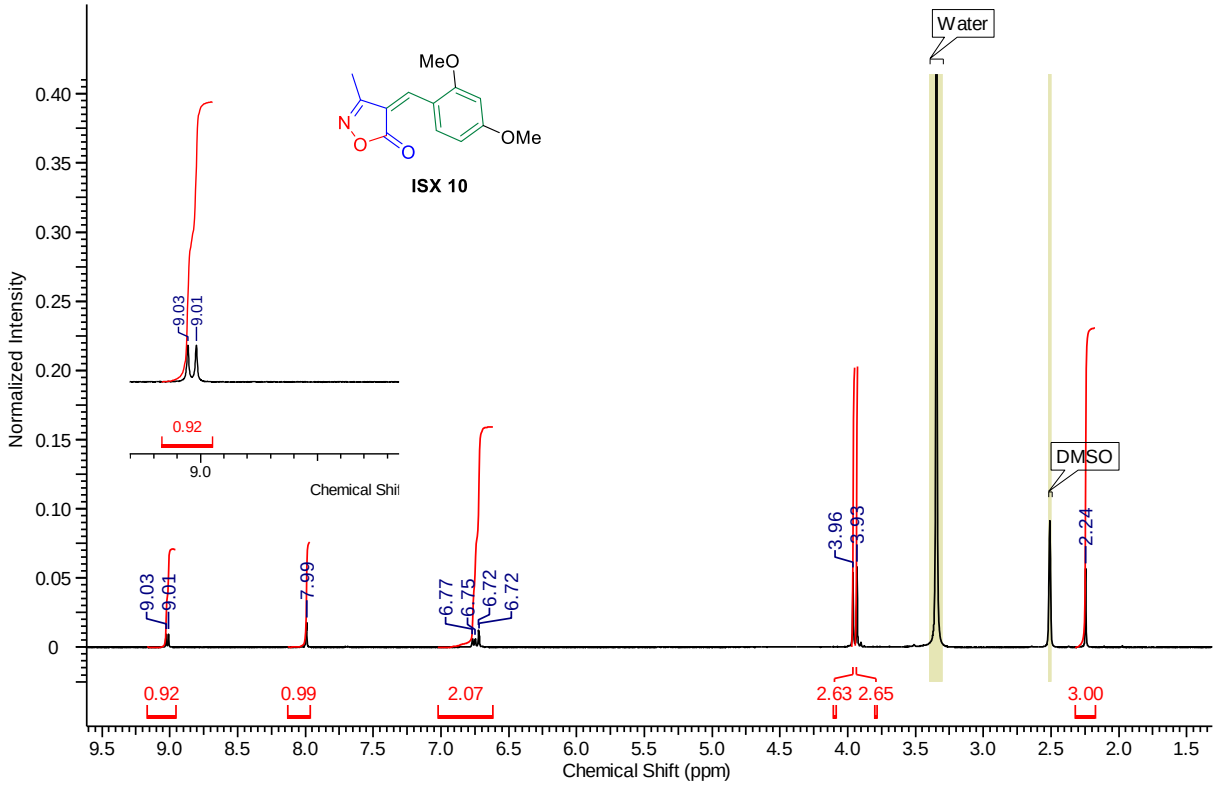

Figure S33. ^{1}H NMR spectrum (500 MHz, $CDCl_3$) of **ISX 10**.

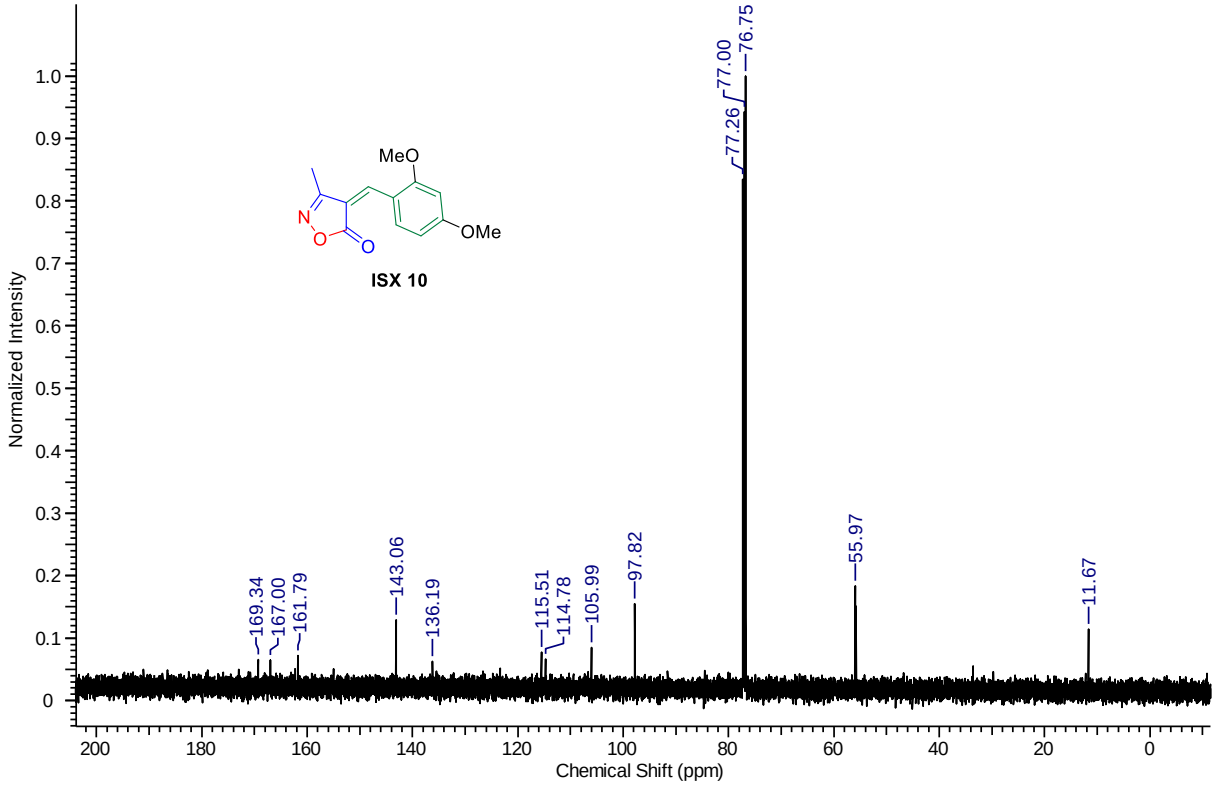

Figure S34. ^{13}C NMR spectrum (125 MHz, $CDCl_3$) of **ISX 10**.

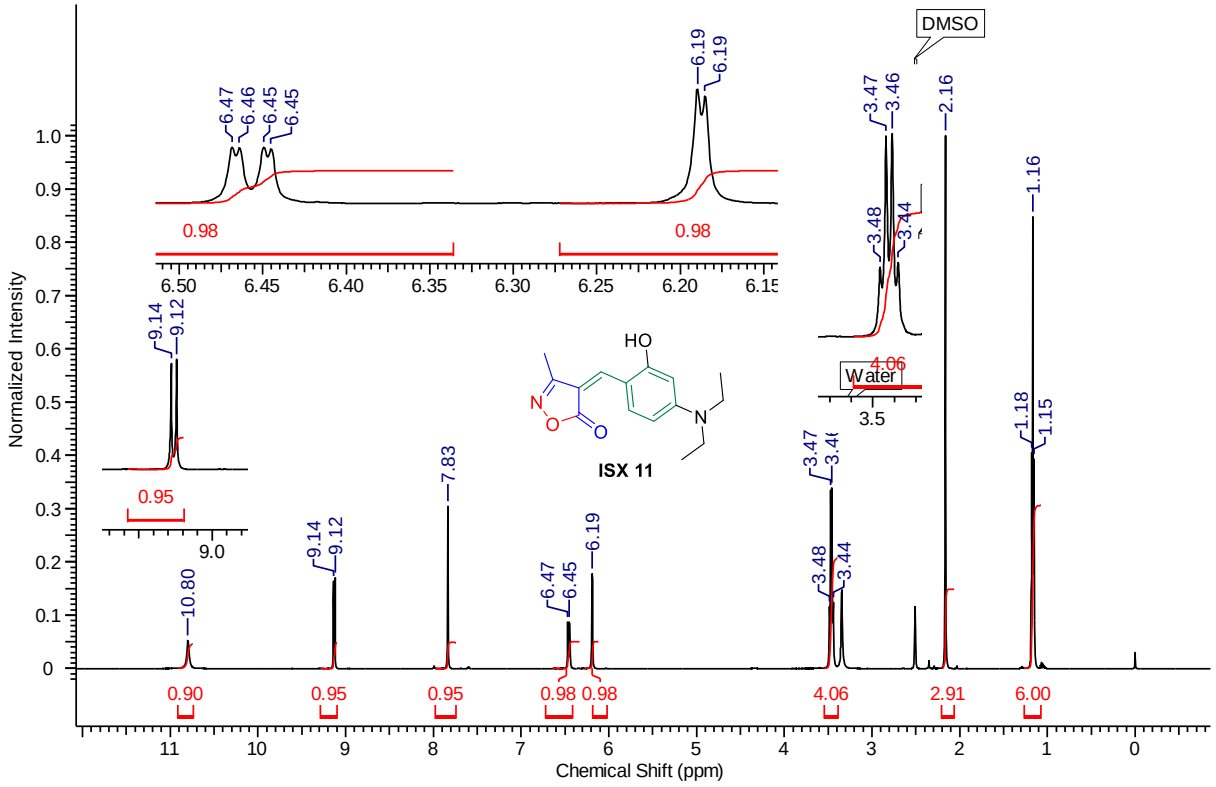

Figure S35. ^{1}H NMR spectrum (500 MHz, DMSO-*d6*) of **ISX 11**.

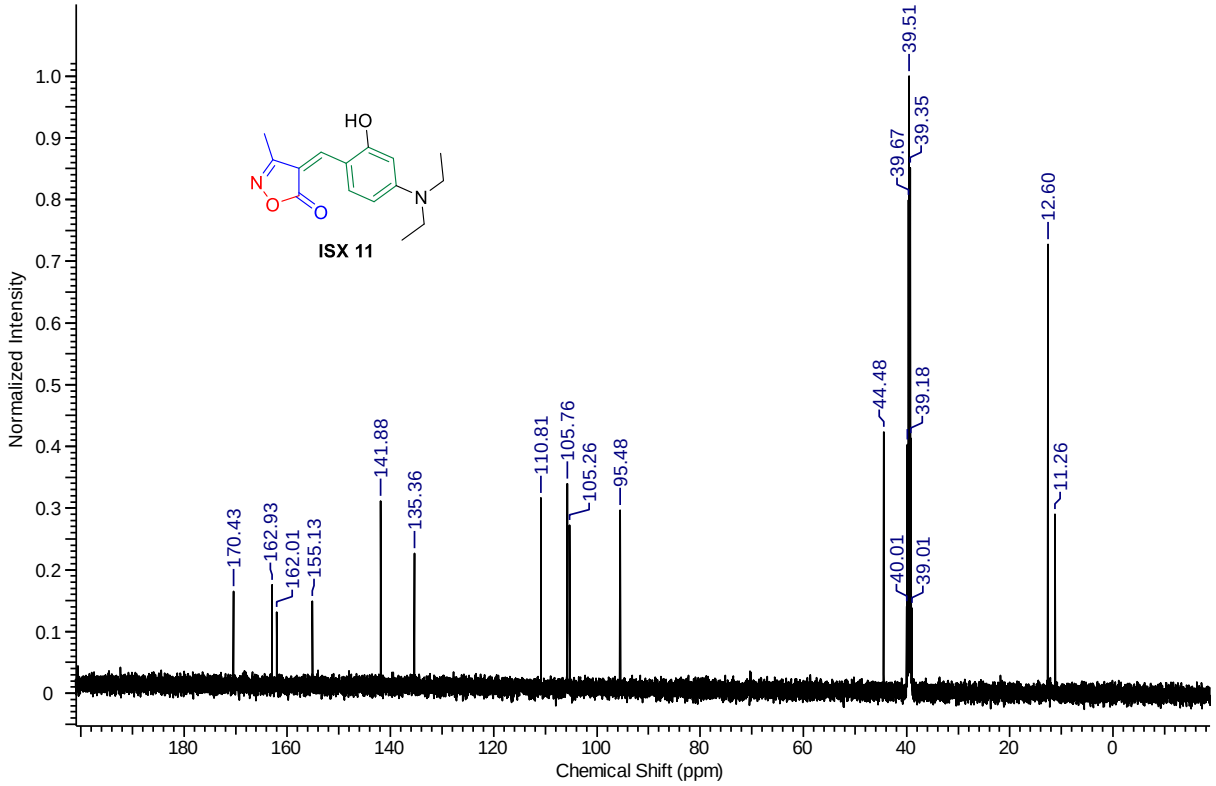

Figure S36. ^{13}C NMR spectrum (125 MHz, DMSO-*d6*) of **ISX 11**.

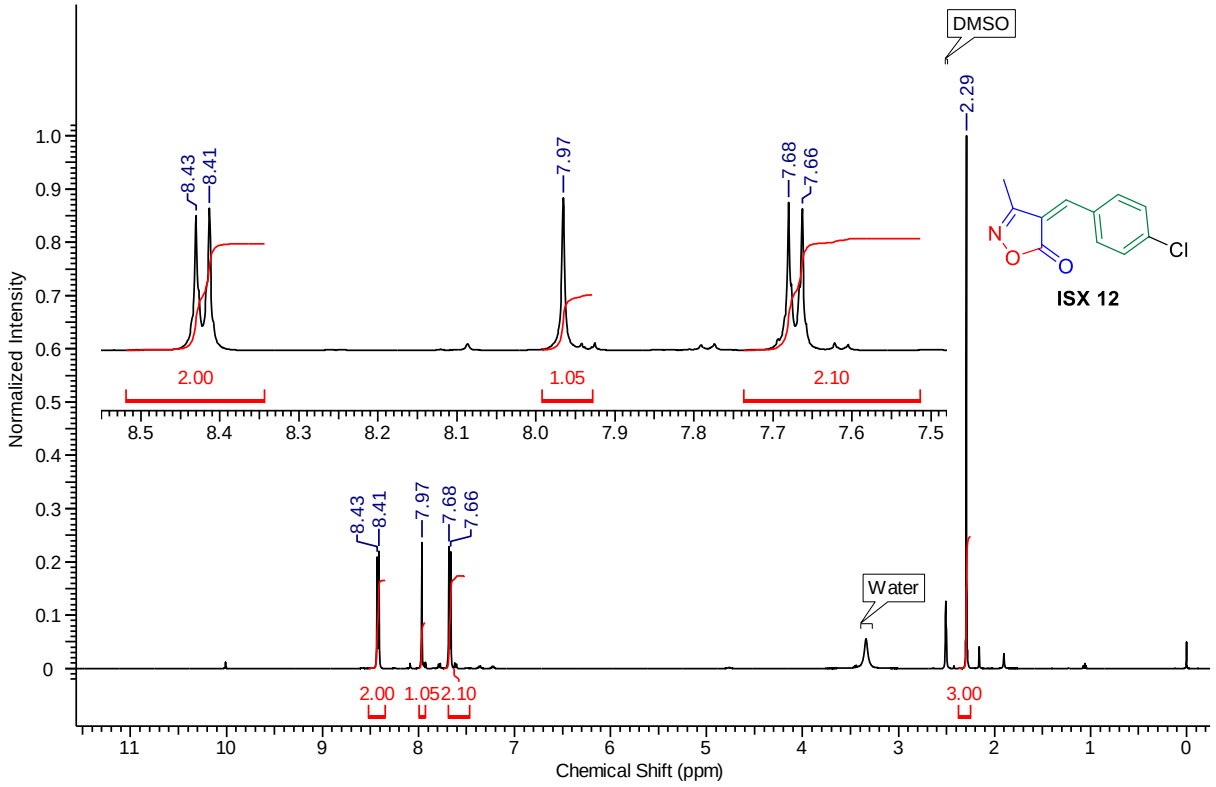

Figure S37. ^{1}H NMR spectrum (500 MHz, $CDCl_3$) of **ISX 12**.

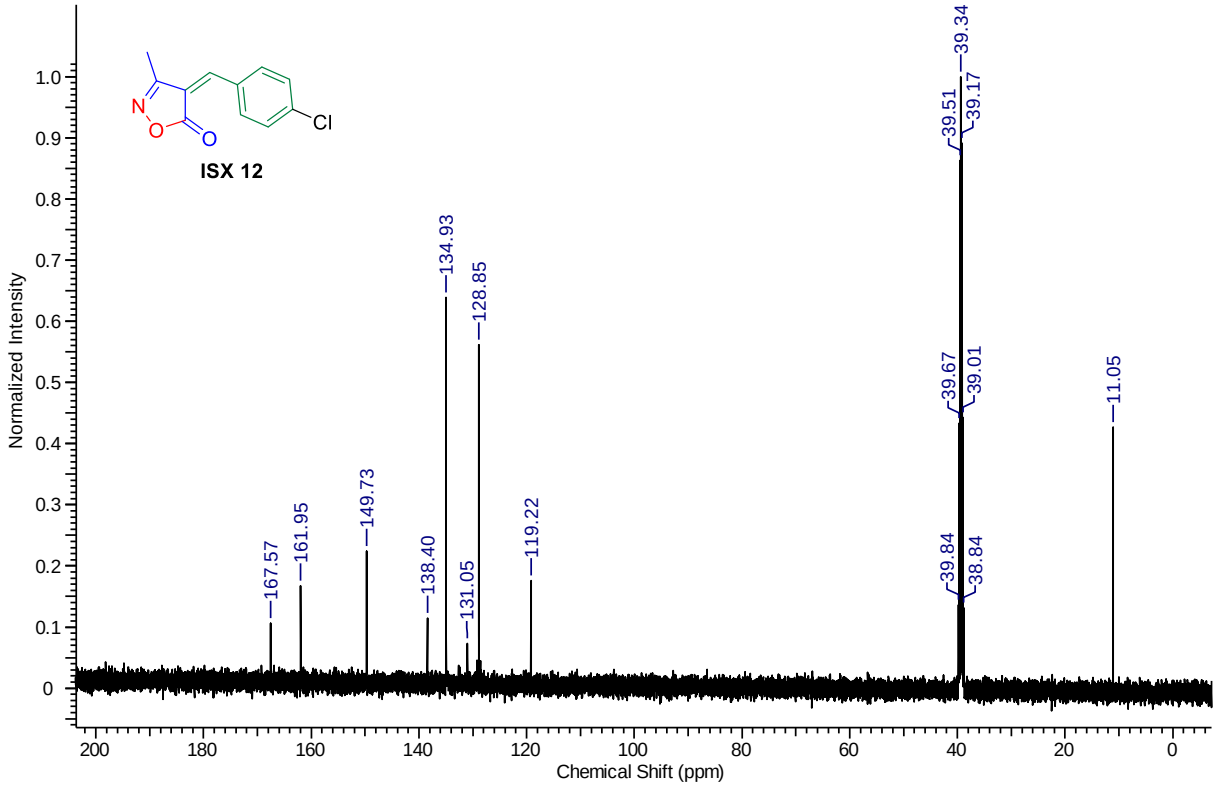

Figure S38. ^{13}C NMR spectrum (125 MHz, $CDCl_3$) of **ISX 12**.

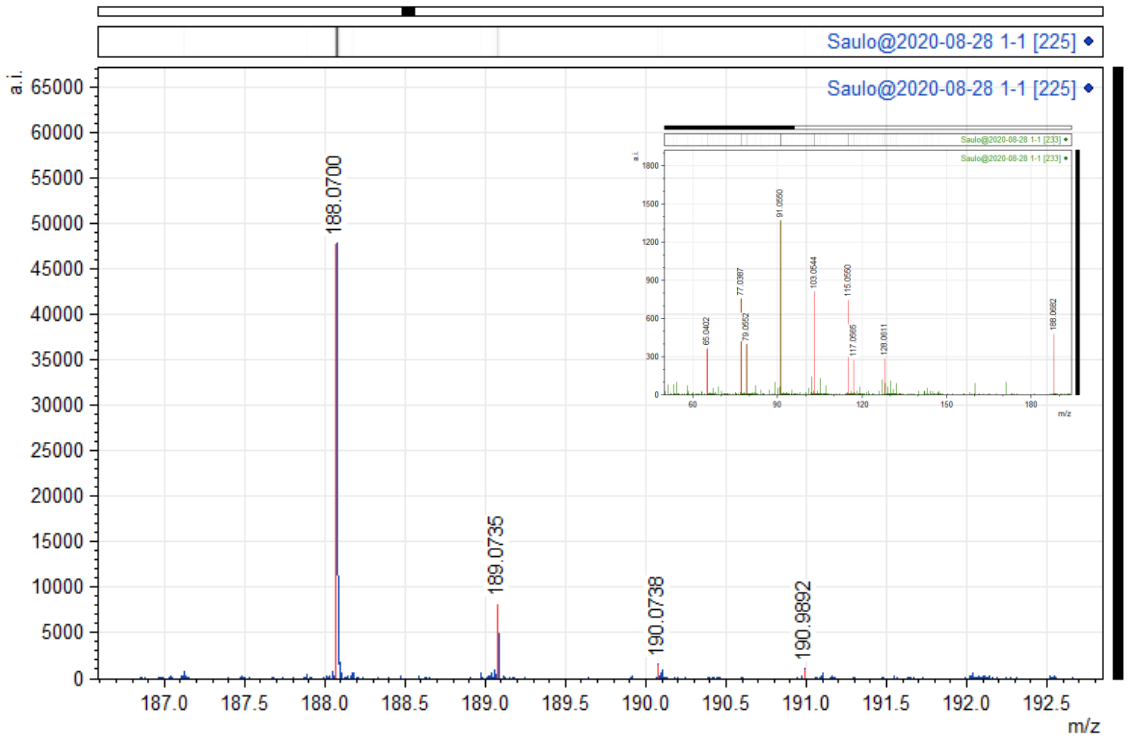

Figure S39. Expansion of the high resolution ESI(+)-MS of the **ISX 01** showing its isotopic pattern. The inset is the ESI(+)-MS/MS from the most intense isotopologue.

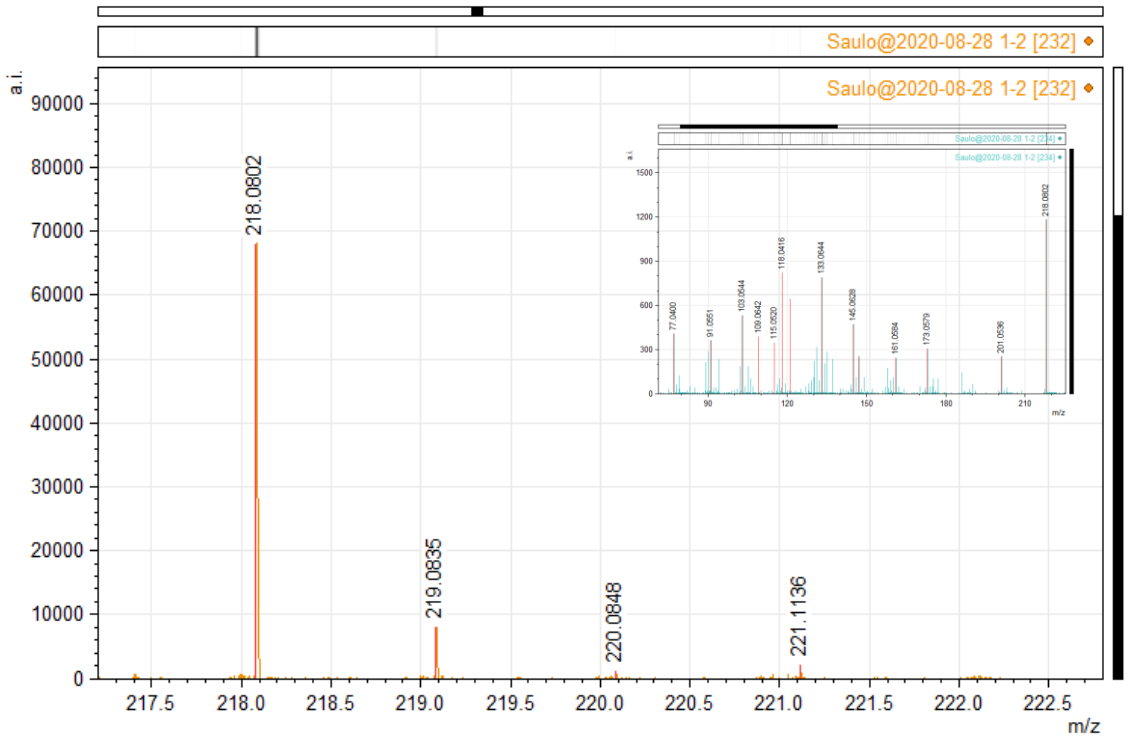

Figure S40. Expansion of the high resolution ESI(+)-MS of the **ISX 02** showing its isotopic pattern. The inset is the ESI(+)-MS/MS from the most intense isotopologue.

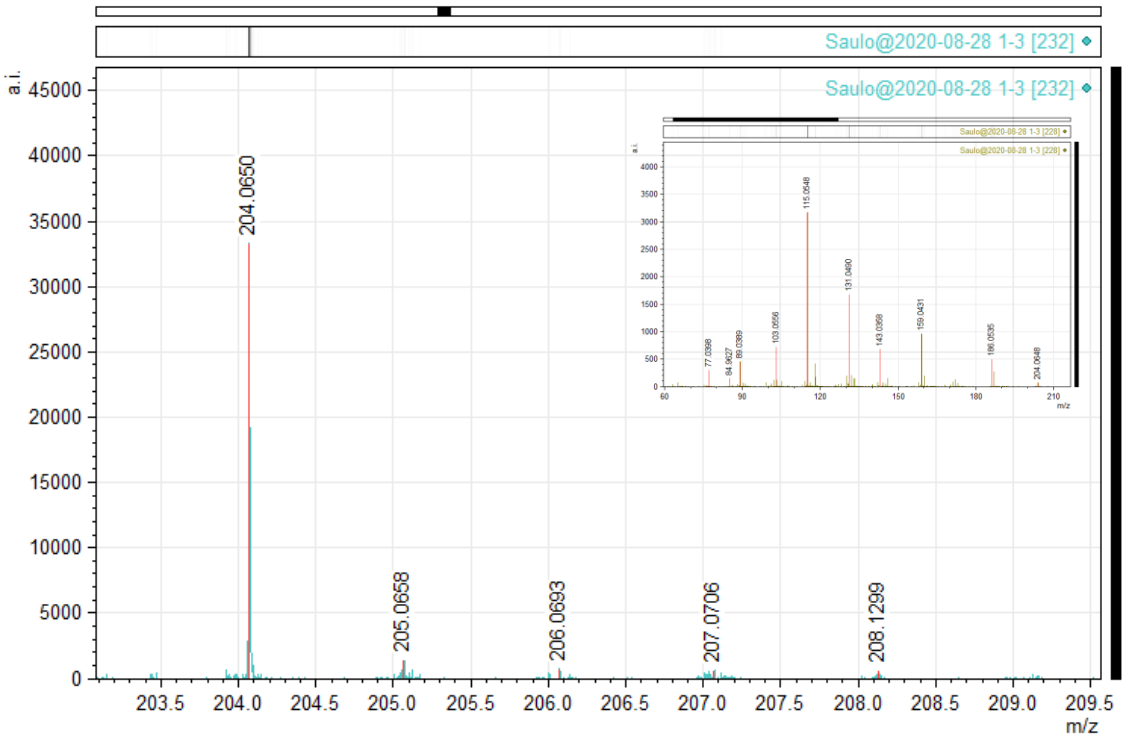

Figure S41. Expansion of the high resolution ESI(+)-MS of the **ISX 03** showing its isotopic pattern. The inset is the ESI(+)-MS/MS from the most intense isotopologue.

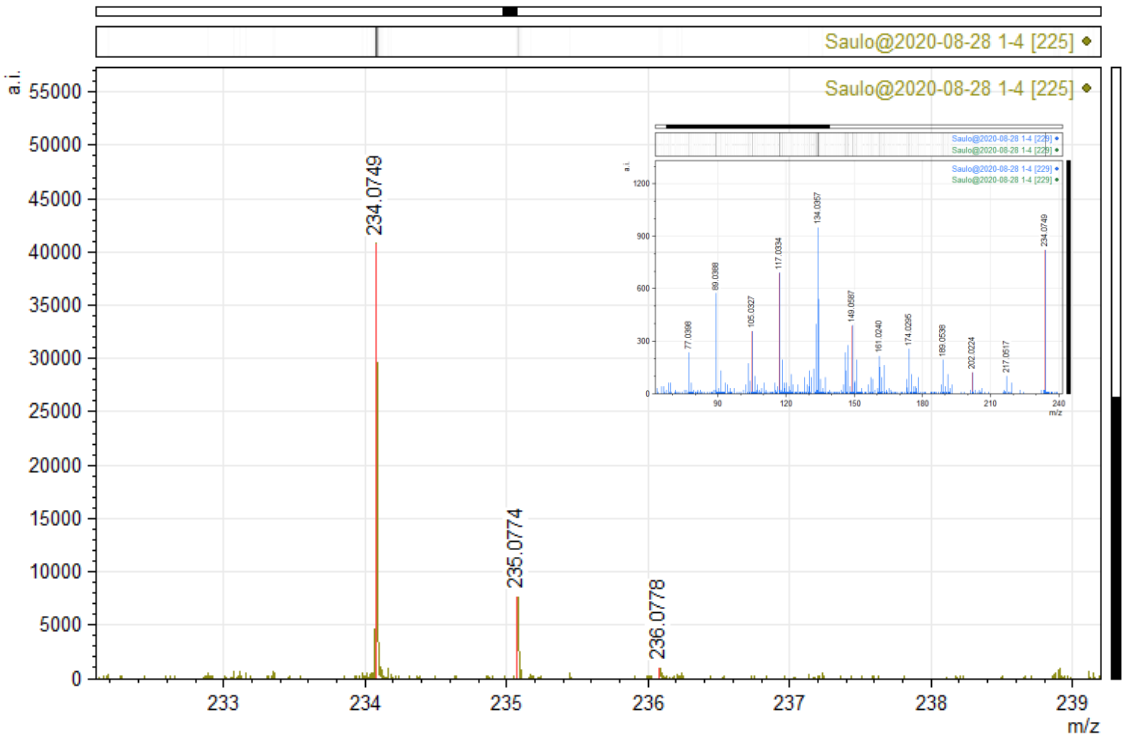

Figure S42. Expansion of the high resolution ESI(+)-MS of the **ISX 04** showing its isotopic pattern. The inset is the ESI(+)-MS/MS from the most intense isotopologue.

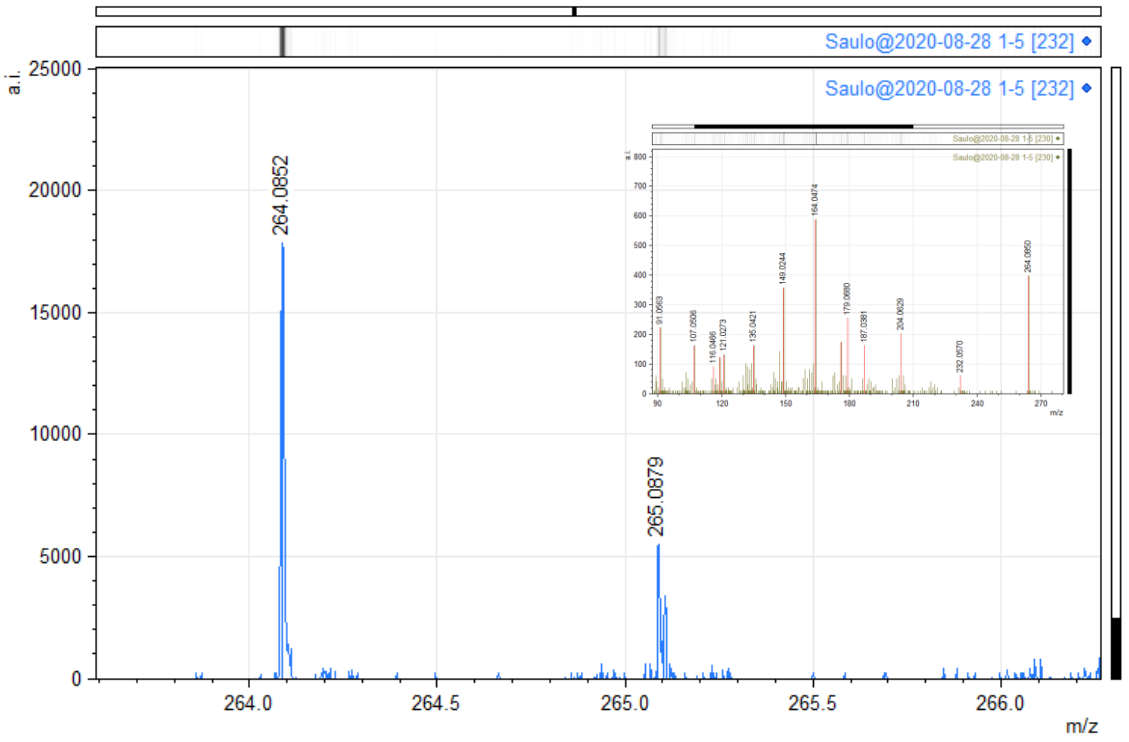

Figure S43. Expansion of the high resolution ESI(+)-MS of the **ISX 05** showing its isotopic pattern. The inset is the ESI(+)-MS/MS from the most intense isotopologue.

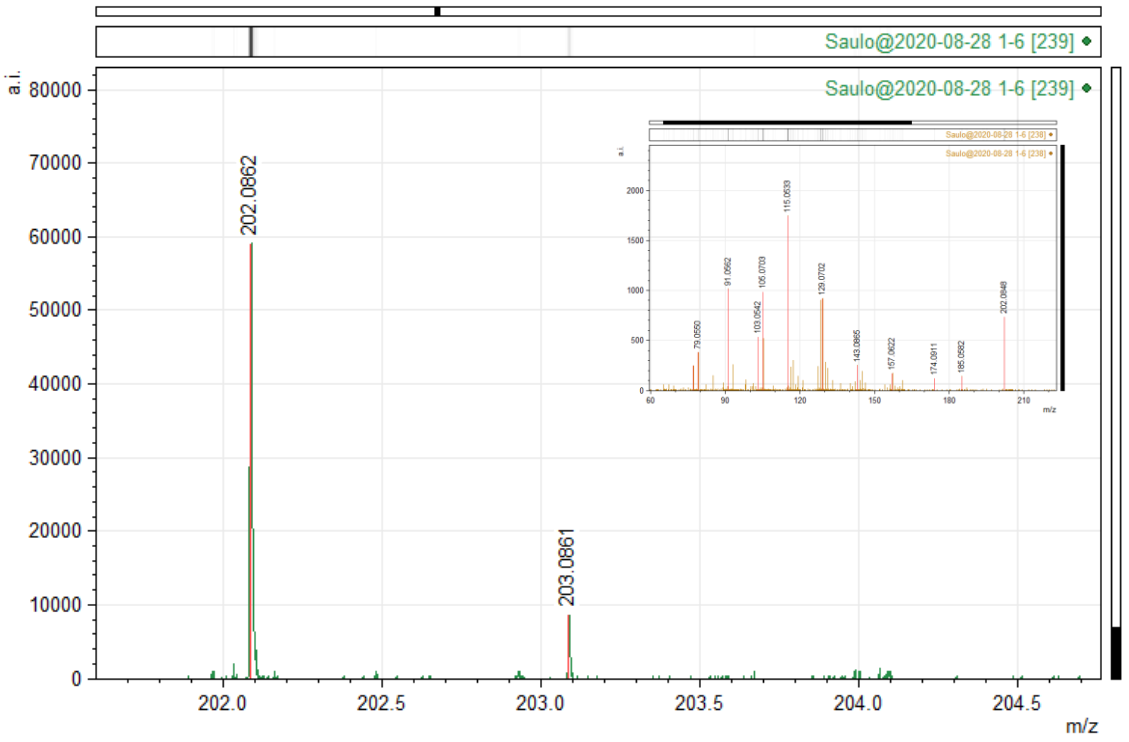

Figure S44. Expansion of the high resolution ESI(+)-MS of the **ISX 06** showing its isotopic pattern. The inset is the ESI(+)-MS/MS from the most intense isotopologue.

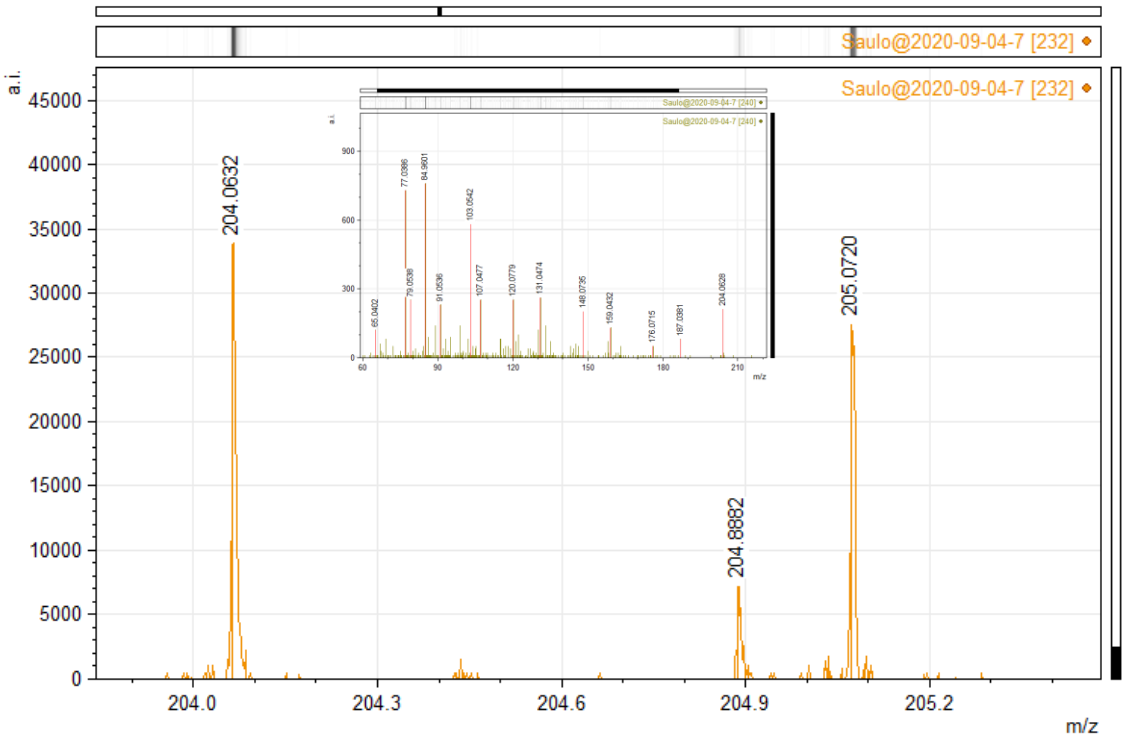

Figure S45. Expansion of the high resolution ESI(+)-MS of the **ISX 07** showing its isotopic pattern. The inset is the ESI(+)-MS/MS from the most intense isotopologue.

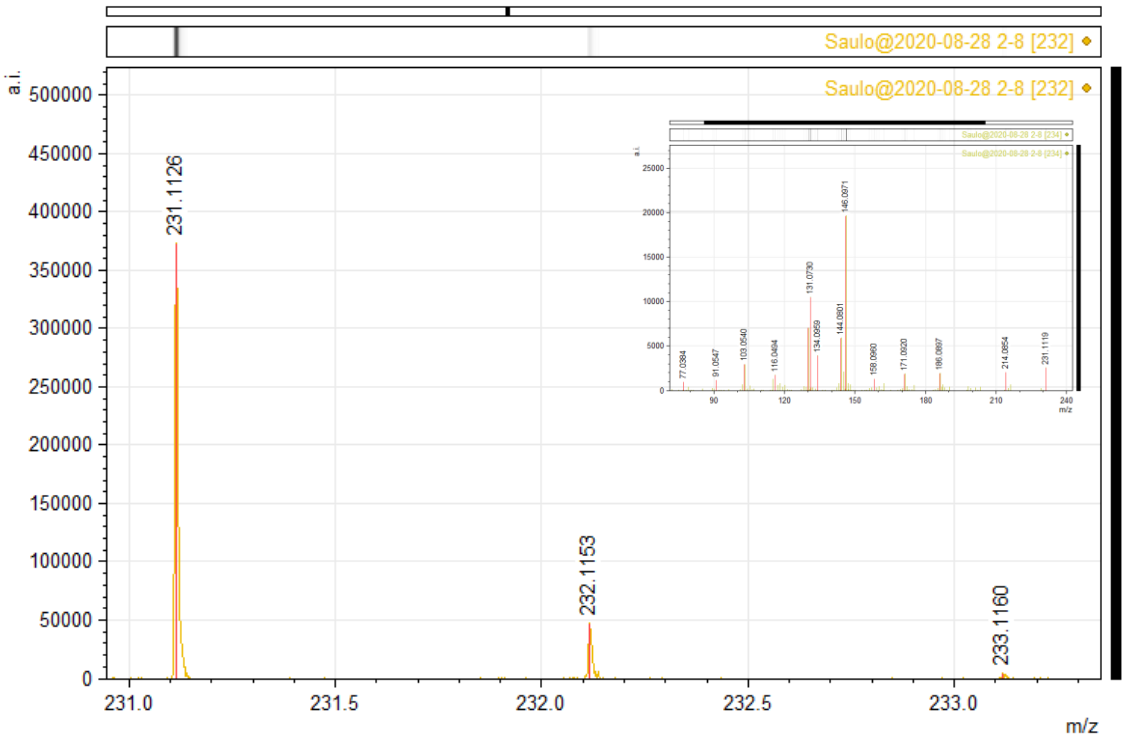

Figure S46. Expansion of the high resolution ESI(+)-MS of the **ISX 08** showing its isotopic pattern. The inset is the ESI(+)-MS/MS from the most intense isotopologue.

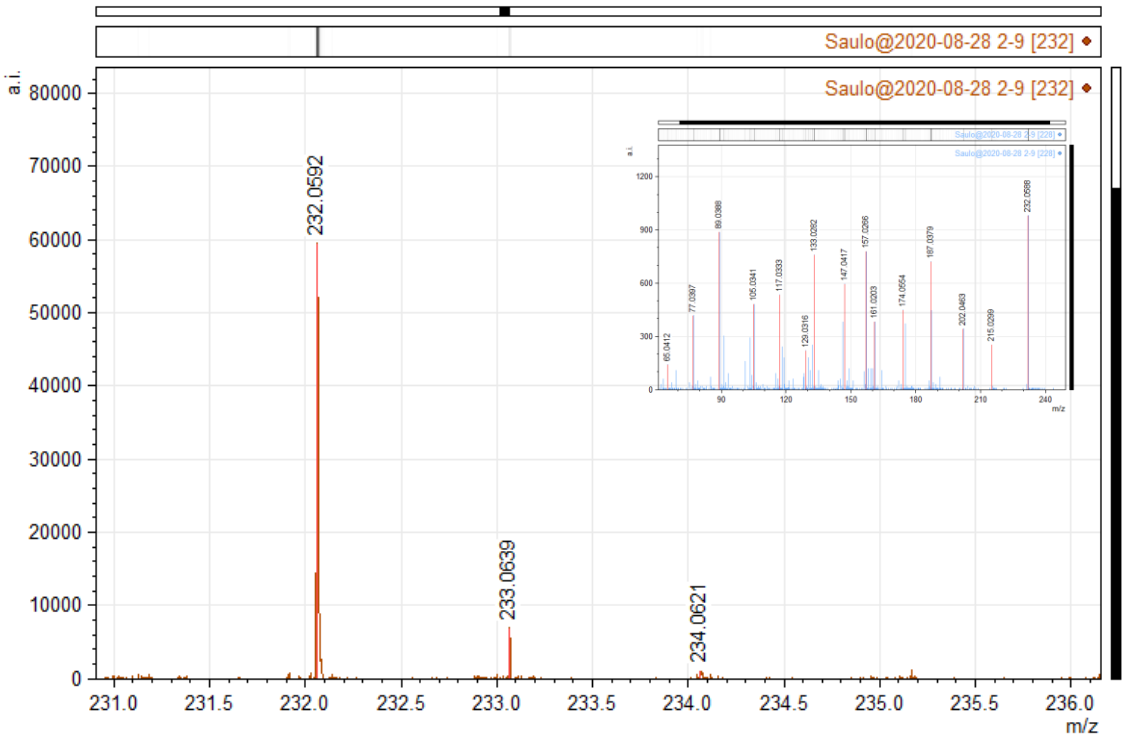

Figure S47. Expansion of the high resolution ESI(+)-MS of the **ISX 09** showing its isotopic pattern. The inset is the ESI(+)-MS/MS from the most intense isotopologue.

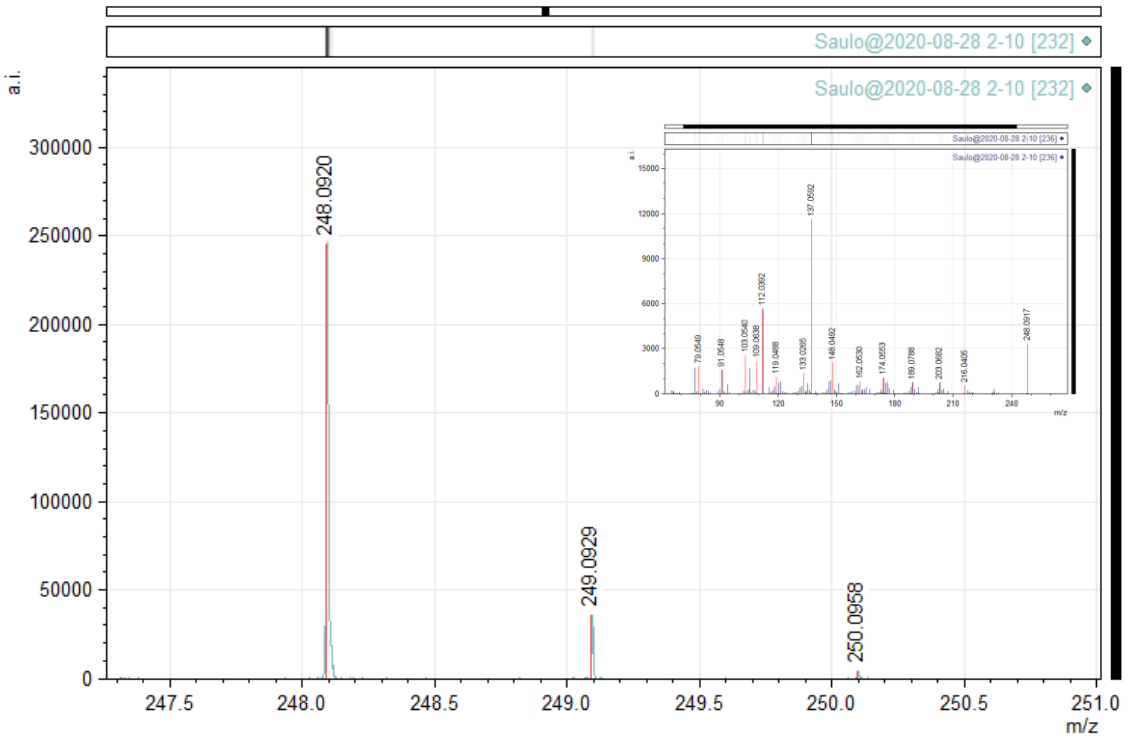

Figure S48. Expansion of the high resolution ESI(+)-MS of the **ISX 10** showing its isotopic pattern. The inset is the ESI(+)-MS/MS from the most intense isotopologue.

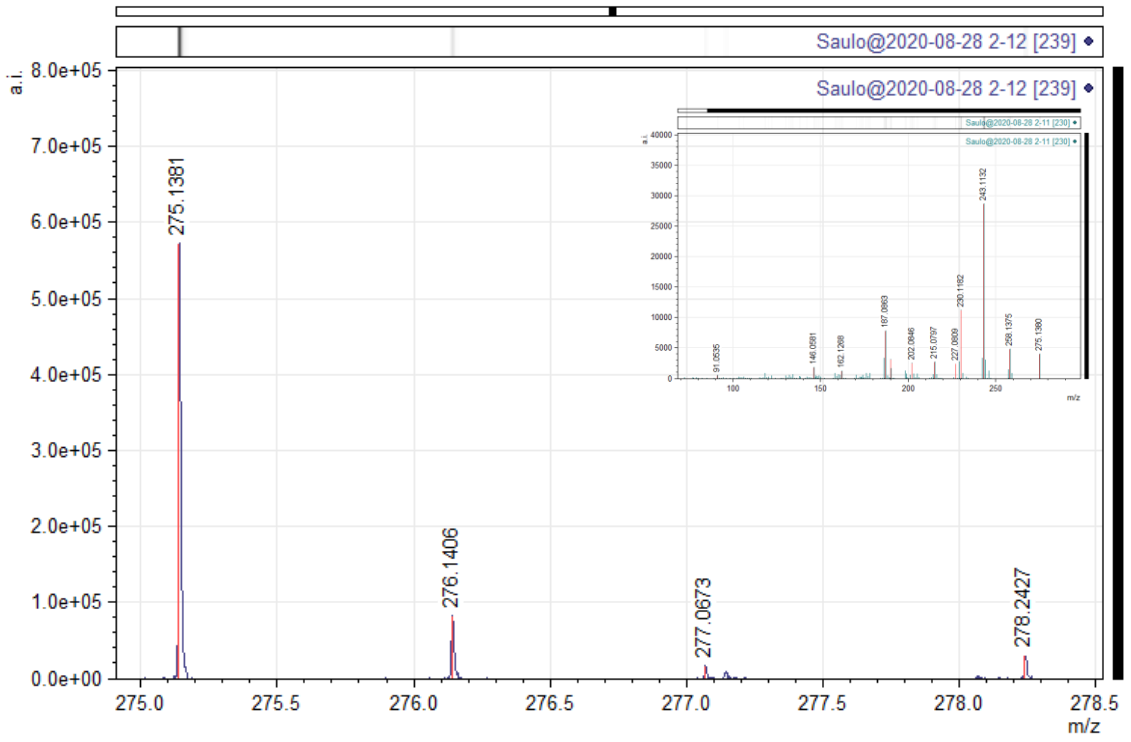

Figure S49. Expansion of the high resolution ESI(+)-MS of the **ISX 11** showing its isotopic pattern. The inset is the ESI(+)-MS/MS from the most intense isotopologue.

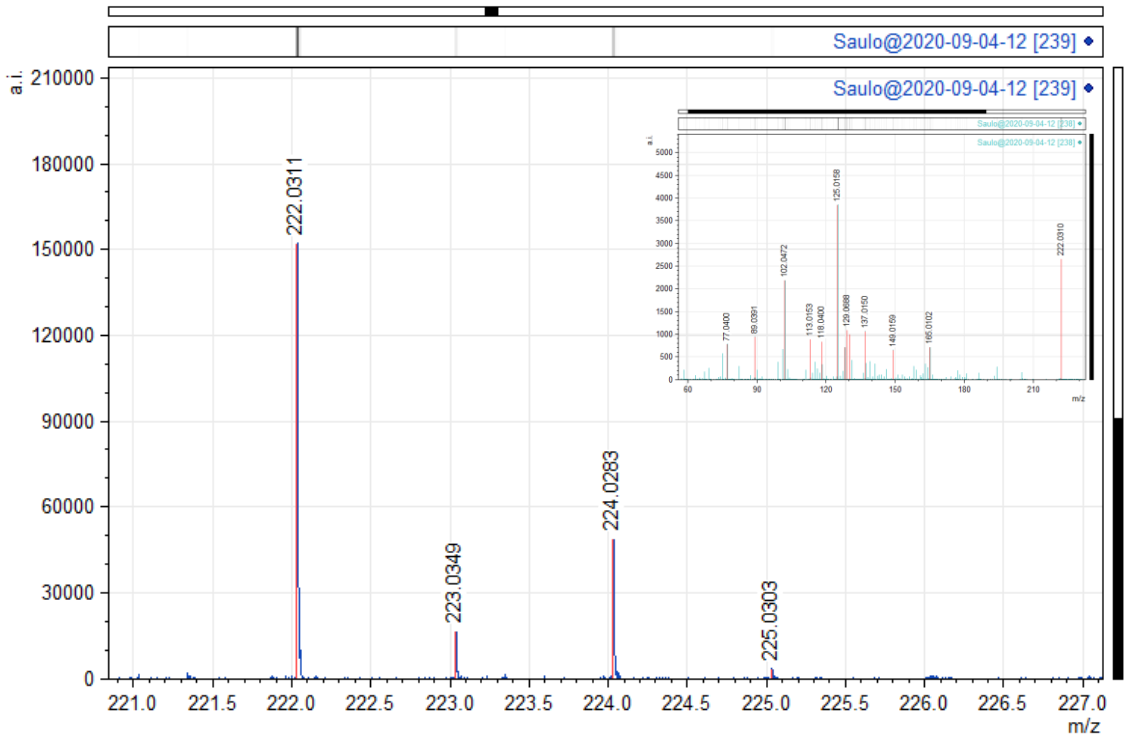

Figure S50. Expansion of the high resolution ESI(+)-MS of the **ISX 12** showing its isotopic pattern. The inset is the ESI(+)-MS/MS from the most intense isotopologue.